# *Meta-analysis of deep neural networks in remote sensing: A comparative study of mono-temporal classification to support vector machines*

Shahriar S. Heydari[a], Giorgos Mountrakis[a1]

[a]Department of Environmental Resources Engineering, State University of New York, College of Environmental Science and Forestry, 1 Forestry Drive, Syracuse, NY 13210, United States

[1]Corresponding author.
E-mail addresses: sshahhey@syr.edu (S. S. Heydari), gmountrakis@esf.edu (G. Mountrakis)

# *Meta-analysis of deep neural networks in remote sensing: A comparative study of mono-temporal classification to support vector machines*

ABSTRACT

Deep learning methods have recently found widespread adoption for remote sensing tasks, particularly in image or pixel classification. Their flexibility and versatility has enabled researchers to propose many different designs to process remote sensing data in all spectral, spatial, and temporal dimensions. In most of the reported cases they surpass their non-deep rivals in overall classification accuracy. However, there is considerable diversity in implementation details in each case and a systematic quantitative comparison to non-deep classifiers does not exist. In this paper, we look at the major research papers that have studied deep learning image classifiers in recent years and undertake a meta-analysis on their performance compared to the most used non-deep rival, Support Vector Machine (SVM) classifiers. We focus on mono-temporal classification as the time-series image classification did not offer sufficient samples. Our work covered 103 manuscripts and included 92 cases that supported direct accuracy comparisons between deep learners and SVMs.

Our general findings are the following: i) Deep networks have better performance than non-deep spectral SVM implementations, with Convolutional Neural Networks (CNNs) performing better than other deep learners. This advantage, however, diminishes when feeding SVM with richer features extracted from data (e.g. spatial filters) ii) Transfer learning and fine-tuning on

pre-trained CNNs are offering promising results over spectral or enhanced SVM, however these pre-trained networks are currently limited to RGB input data, therefore currently lack applicability in multi/hyperspectral data. iii) There is no strong relationship between network complexity and accuracy gains over SVM; small to medium networks perform similarly to more complex networks. iv) Contrary to the popular belief, there are numerous cases of high deep networks performance with training proportions of 10% or less.

Our study also indicates that the new generation of classifiers is often overperforming existing benchmark datasets, with accuracies surpassing 99%. There is a clear need for new benchmark dataset collections with diverse spectral, spatial and temporal resolutions and coverage that will enable us to study the design generalizations, challenge these new classifiers, and further advance remote sensing science. Our community could also benefit from a coordinated effort to create a large pre-trained network specifically designed for remote sensing images that users could later fine-tune and adjust to their study specifics.

KEYWORDS:

Deep learning, classification, Convolutional Neural Network, Deep Belief Network, Stacked Auto Encoder, Support Vector Machine

## 1. INTRODUCTION

Artificial neural networks (ANNs) first started with cybernetics in the 1940s–1960s and led to the invention of the first single neuron model named perceptron (Rosenblatt, 1958). Being a data-driven model with the ability to simulate arbitary computing functions through optimization, ANNs found a wide range of applications. The next major breakthrough happened in late 80's with the invention of back-propagation and a gradient-based optimization algorithm to train a neural network with one or two hidden layers with any desired number of nodes (Rumelhart et al., 1986). The back-propagation method has worked well for non-deep structures (1-2 hidden layers) but gradient-based training of deep neural networks (DNNs) could get stuck in local minima or plateaus due to the dramatic increase in number of model parameters and vanishing of gradients during backpropagation (Bengio, 2009). There is no standard definition to label a neural network as deep, but it mostly refers to network of two hidden layers or more, used to automatically extract a hierarchical set of features from data. Compared to 1-2 layer structures, DNNs promise to provide more compact models for the same modeling capabilities (Bengio, 2009). However, the high node number of DNNs made it difficult to train and optimize in a practical manner.

The seminal work of Hinton et al. (2006) showed that unsupervised pre-training of each layer, one after another, could considerably improve results. This layer-wise training approach, named greedy algorithm, was the key that opened new avenues to deep neural networks. The greedy algorithm could also be followed by a fine-tuning process, in which the entire network is tuned together using backpropagation, but this time from a much better starting point. Deep network theories and practices have expanded considerably during the last decade. It has resulted in establishment of some major network types (with continuous enhancements) and numerous

applications in different domains. In close relationship with image processing and computer vision, remote sensing (RS) is one of many areas that deep learning is targeting.

Generally and following discussion in L. Zhang et al. (2016), we can categorize remote sensing applications of deep learning into four groups: 1) RS image pre-processing, 2) scene classification, 3) pixel-based classification and image segmentation, and 4) target detection. For image pre-processing tasks, we can name pan-sharpening, denoising, and resolution enhancement as major applications. Scene classification is done based on some extracted features from a scene, which the deep networks are assumed to be good at. The non-deep approaches normally use some handcrafted features extracted from the scene to feed the classifier (SVM, KNN, etc.) and predict the scene type. Deep networks have opened the door to direct use of spectral and spatial information together to generate a richer set of features automatically. This automatic extraction increases the potential for good generalization and scalability of this method compared to handcrafted features. Handcrafted features tend to be tailored closely to a specific case and application and possibly perform better than any automatic system, but because of this specificity they cannot be easily or successfully generalized to another cases/studies. This type of work is closely related to image recognition task but for categorization of remote sensing scenes (such as agricultural field, residential area, airport, parking lot, etc.), therefore sharing network configurations between computer vision and remote sensing applications is common here. Pixel classification and segmentation (or semantic labeling) are similar to scene classification but operate at the pixel rather than scene level, and produce a thematic map instead of a single category index. This is perhaps the most studied RS application and deep networks have shown performance benefits due to their ability to co-process spatial and spectral data easily, especially for hyperspectral images. Our main target in

this paper is to focus on image or scene classification - we do not address other applications. In addition, we focus on mono-temporal classification as the time-series image classification is still in its infancy. Target or object detection is generally an extension to the three aforementioned groups, where specific objects defined by their shape or boundary are extracted from an image. This field has found many useful but challenging applications in high resolution and real time image/video processing.

Following the explosive growth of new algorithmic developments and case studies in deep learning RS applications in the past 3-4 years, several review manuscripts have been published (Ghamisi et al. (2017), Xia et al. (2017), L. Zhang et al. (2016), or P. Liu et al. (2017)). The majority of these reviews are descriptive and do not offer a quantitative assessment of deep learning benefits building on the extensive available comparisons in the literature. The overal goal of this work is to bridge this knowledge gap by undertaking a meta-analysis comparing deep and non-deep classification algorithms through a meta-analysis of published research.

Other meta-analysis works exist but they do not examine explicitly deep learning benefits. For example, Khatami et al. (2016) grouped all neural network types under one category and did not distinguish deep networks from other implementations. Ma et al. (2017) conducted similar meta-analysis focusing on object-based classification (thus excluding pixel-based ones) without separating deep learning methods. There are some other papers that review deep learning architectures in general such as Deng (2014) or W. Liu et al. (2017), or for specific type of data, such as Camps-Valls et al. (2014) on hyperspectral data classification. These works also lack quantitative comparisonsusing a meta-analysis approach.

The overarching goal is to provide readers with the “big picture” of current research and build on the collective knowledge of published works to assess deep learning benefits in remote

sensing. To undertake the proposed meta-analysis task, we reviewed major research papers and built a database of case studies of deep network applications in the remote sensing field while extracting main network and data characteristics. This database was analyzed to identify deep learning classification performance and its distribution across these network (e.g. network complexity) and data characteristics (e.g. spatial resolution). We expect this analysis to provide a knowledge baseline as the remote sensing community further incorporates deep leaning in related activities.

The structure of the manuscript is as follows. A brief overlook of deep network types is presented in section 2 along with key introductory references. A summary table is also provided to describe extracted parameters for each research paper. In section 3 after introducing a descriptive statistics and summarizing design ideas encountered in the selected resesrch papers and used datasets, we provide our main comparative analysis and discuss important research questions about parameters effect on network performance. The last section provides concluding remarks.

## 2. METHODS

In this section we first describe three DNN methods that have been popular in RS tasks. Section 2.2 contains an explanation on the paper database and associated characteristics and metrics used in the comparative accuracy analysis between DNNs and non-deep methods.

### 2.1. Summary of popular deep neural networks in remote sensing

The deep learning paradigm is concentrated on automated hierarchical feature extraction. Numerous methods and their modifications have been devised along the past years. Here we

140 briefly introduce the three most widely used structures which were used in our identified studies.
141 More detailed descriptions of each structure can be found in many machine learning textbooks,
142 for example Bengio (2009) and Goodfellow et al. (2016), or tutorials such as Le (2015) and
143 Deng (2014). Zhu et al. (2017) and L. Zhang et al. (2016) also provide tutorials for deep learning
144 for remote sensing (RS) applications.

145 Deep networks have been developed to enhance and enrich data representations in an
146 automated and intelligent manner. A good representation is, of course, dependent on the specific
147 application and should be learned from training data. One important deep network category in
148 this class is based on Autoencoders (AEs). The idea behind an autoencoder is basically an
149 encoder-decoder network to regenerate the input as accurately as possible in its output. Under
150 specific conditions, the encoder part works as a good feature extractor and can be stacked to
151 build deep networks named Stacked Auto Encoders or SAEs (the decoder part is not used). The
152 imposed condition on objective function is typically a form of sparsity, but other variants are also
153 studied. To put it simply, AE learns a deterministic representation of the input by minimizing a
154 cost function based on the difference between input and the regenerated one at the decoder
155 output. This learning takes place using gradient-based optimization and standard
156 backpropagation techniques. AEs are well suited to unsupervised learning and can be trained
157 layer-wise, possibly followed by a supervised fine-tuning phase of the entire network. For a good
158 overview of autoencoders with some work examples and executable codes see Andrew Ng's
159 Deep Learning tutorial at http://deeplearning.stanford.edu/wiki/index.php/UFLDL_Tutorial.
160 Vincent et al. (2010) also provide more details on autoencoders and unsupervised learning.

161 Another way of thinking about data representation is to learn the statistical distribution of
162 input, i.e. a probabilistic approach. This approach has led to Generative models or Structured

Probabilistic Models. Deep belief network (DBN) based on stacking layers of Restricted Boltzmann Machine (RBM) is the most popular variant for RS applications. Here the aim is to minimize the Boltzmann cost function, to maximize "the similarity (in a probabilistic sense) between the representation and projection of the input" (Singhal et al., 2016). This optimization does not use an assumed output, so a different algorithm (contrastive divergence) is required to train the neurons. However, similarly to the autoencoder, training is unsupervised and, more important, it can be done in a greedy layer-wise approach for a stack of layers. This layer-wise approach was devised by the seminal work of Hinton et al. (2006) and later implemented by both SAEs and DBNs. Therefore SAEs and DBNs are often discussed together in the literature (e.g. Vincent et al. (2010)). When trained, the network can provide extracted features for the new data to be classified. Tutorials on RBM and DBN are available through the internet, for example see https://deeplearning4j.org/restrictedboltzmannmachine, which includes executable codes.

The third type, which is the most used structure in recent years, is the convolutional neural network (CNN). Inspired by the human visual system and designed to process images, it has limited connection to only adjacent neurons in each layer, with the same connection weights for each neuron within each layer. It may include down-sampling in each layer, which reduces the processing resolution but adds translation invariance property to the network. Each layer's output is typically named a map and it is generally desired to have multiple maps generated at each layer. Here the filter weights are tuned typically by supervised training, as the limited number of shared parameters in each layer (compared to a fully connected network) allows it. There are also some pre-trained large network structures publicly available for use and fine-tuning them for specific applications is another common approach. For a university course on convolutional

185 neural networks readers are referred to http://cs231n.stanford.edu/. Zeiler and Fergus (2014) also
186 provide a discussion on visualization and understanding of the internal CNN workings.
187 Working with sequence data is another important type of remote sensing works, particularly
188 on three bases: studying hyperspectral signal variations and analyzing their dependencies; adding
189 the time dimension as another data element to explore land use feature patterns (profiles) and use
190 them in classification; and pursuing detection of changes in land cover or land use by processing
191 time-series data. Neural networks – and specifically Recurrent Neural Networks – are gaining
192 momentum for these applications but the number of published papers is still low. These
193 networks are promising with new modifications such as adding more powerful and deep memory
194 cells (see for example Lyu et al. (2016), Mou et al. (2017), Rußwurm and Körner (2017),
195 Rußwurm and Körner (2018), Ndikumana et al. (2018), Niculescu et al. (2018), or Sharma et al.
196 (2018)). However, we did not consider sequence data applications in our paper due to lack of
197 enough data and our focus was only on feed-forward networks and its three main variants: SAE,
198 DBN, and CNN.
199
200 2.2. Comparative performance database creation
201 Our overarching goal is to look at the analyzed DNN case studies and compare them together
202 and to a well-known non-deep classifier, Support Vector Machine (SVM). SVM will serve both
203 as a representative for non-deep classifier to compare with deep networks, and as a baseline to
204 compare different DNN architectures. SVMs were selected as the benchmarking algorithm
205 because: i) they were found to be the best non-deep performing classifiers in an extensive
206 comparison of published work (Khatami et al., 2016), and ii) the majority of DNN papers found
207 in this review chose to include SVM as the main benchmark, thus validating our decision. We

also examine accuracy trends across data and method characteristics. Direct comparisons of published works are not feasible due to variances in data types, sampling design, algorithmic details, and test metrics. Therefore, we concentrated on aggregating results from manuscripts where accuracy metrics are reported mutually under common conditions for deep and non-deep implementations. This database was then used to do comparative meta-analysis and other quantitative statistical analyses.

The result was 103 research papers from 2014 until Nov. 2018 covering 183 case studies that include deep learning-based classification, 92 cases of which supported direct comparisons of accuracy to SVM. The main characteristics of these case studies are summarized in Table A1, Appendix A, with each column of the appendix table defined in Table 1 below. These parameters reflect the most important aspects of the research design and we use them to present the discussion of our research questions in the subsequent sections. We treat each data set in a research paper as a separate case, because the output result and possibly the network structure may vary per case in any single paper.

225 Table 1: Parameters collected on each case study
226

| | |
|---|---|
| Reference | Citation code for the referenced research paper |
| Network Type | One of below categories:<br>- Convolutional Neural Network (CNN),<br>- Deep Belief Network (DBN),<br>- Stacked AutoEncoder (SAE) |
| Learning strategy | One of below categories:<br>- Unsupervised<br>- Unsupervised & fine-tuning<br>- Semisupervised<br>- (fully) Supervised<br>- Transfer learning<br>- Transfer learning & fine-tuning |
| Number of parameters | Number of trainable network parameters, i.e. weights and biases of network neurons and connections. We manually created this number to approximate network complexity. |
| Dataset | Name of dataset used for the research, including:<br>- Brazilian coffee, NWPU-RESISC45, RSSCN7, UC Merced, and WHU-RS19: 3-band images used in scene classification,<br>- Indian Pines, Houston, Kennedy Space Center, Pavia University, Pavia City Center, and Salinas: hyperspectral images used in pixel classification,<br>- ISPRS Potsdam and ISPRS Vaihingen: very high resolution images used in image segmentation,<br>- Others: Remaining datasets. |
| Spatial resolution | Dataset spatial resolution expressed through pixel size. |
| # of channels | Number of spectral and auxiliary channels. |
| Training proportion | Proportion of training data size in reference dataset. |
| Metric type | Metric used for reporting performance in research case, including Overall Accuracy, Average Accuracy, Average Precision, F1, Kappa, etc. |
| Deep network result | Best reported value of network classification performance |
| SVM results | Best achieved performance of SVM implementation |

227
228 One of the most important parameters in network specification is the number of network
229 parameters which reflects network complexity. This is typically a surrogate of network depth and
230 width. It is expected that a bigger network would be more powerful, but the network architecture

and way of processing (reflected in other columns of the table) greatly impacts this performance. Therefore, it is not unexpected that a smaller but more elegant network outperforms a larger one in obtained accuracy. For example, in classifying the ISPRS Potsdam and Vaihingen datasets, Maggiori et al., (2016) achieved > 1% better accuracy than Volpi and Tuia (2017) by a network having around $1/10^{th}$ of their network size. This number is mostly calculated from network parameters given in the cited paper but in some cases it is given in the cited paper as well. In cases that given information was not sufficient or ambiguity was not cleared by correspondence, the entry was left blank. This number includes parameters in as many network branches as implemented, but it does not include parameters associated with additional stages of combination or fusion with other data or algorithms. It also counts the network layers parameters up to the last layer before the final classifier, which is typically a Softmax layer but SVM is also used. In around 70% of our cases the deep network is followed by a Softmax classifier, therefore we drop the final classifier type from our list of parameters.

The learning strategy column is another important network parameter. It does not point to the final classifier training as it is always supervised, but shows the methodology for determining network parameters. The supervised learning is the most common approach in deep networks. It can also have different variations in the form of cost function or optimization procedure, or being enhanced by data-driven techniques such as active learning. Those advanced cases are designated as supervised+ in our database. The fine-tuning options show the cases when network parameters are fine-tuned after an initial unsupervised learning or transferred from a pre-trained network in transfer learning. Transfer learning is available to CNN only. DBNs are usually limited to unsupervised & fine-tuning type, while SAEs are used with both unsupervised learning

253 techniques. Semi-supervised learning is also used in some cases, which is a strategy for using
254 both labeled and unlabeled data in optimizing the network cost function.

255 Spatial resolution in our collected research cases varies from 5cm for VHR imagery to 30m
256 for Landsat, left blank if not provided. The number of channels shows the ones that have been
257 actually used in the experiment (some channels have been set aside for their low quality in some
258 studies but not in the others). Note that in some cases the input channels are processed and
259 dimensionality was reduced (mostly employing PCA) and the result is applied to the network,
260 but we do not mention this dimensionality reduction in the table, although we take it into
261 consideration when calculating the number of parameters and consider the network in its actual
262 tested configuration. There are two cases of using Landsat and one case of MODIS imagery that
263 has been indicated in table separately due to importance of these data sources Although from one
264 hand they are of less attention today because of their inferior spatial resolution, but from the
265 other hand they are of interest for their rich temporal dimension in time-series analysis. Data
266 fusion from different sources is also experiencing growing attention, especially adding height
267 data through digital elevation models (DEM). We discuss this further in the design options
268 (section 3.3) but an in-depth analysis of this issue was outside the scope of this work.

269 Another important factor in network prediction performance is the data training size. More
270 training data typically leads to better network generalization, but in many cases the labeled
271 training data is very limited. The corresponding column shows the rounded proportion of
272 (labeled) training data samples to the entire reference data set, varying from as low as 0.1% to
273 90%. We refer to it as “training proportion” hereafter, and consider the proportion in one single
274 run of the network, therefore a cross-validation scheme does not change the value in the table
275 from a similar hold-out.

The reported classification accuracy (overall or average) value is the best performance reported for the reference dataset in each case. It is reported as a number between 0-100 except for the metric Average Normalized Modified Retrieval Rank (ANMRR). Although overall accuracy is an aggregate metric and cannot show important class-dependent performance values, but it is still the most widely used metric due to its simplicity and general applicability. Even though in some cases more detailed evaluations are provided along with overall accuracy, due to different experimental designs and data structures in our meta-analysis, these detailed metrics were not widely comparable and therefore class-specific measures were not included.

In some cases, an additional pre- or post-processing step complements the deep network to enhance the performance, for example merging the resulting map with an auxiliary segmentation result, adding a conditional random field (CRF) layer for edge enhancement, or object-based processing. These methods differ largely in implementation details and experiment setup so cannot be directly compared to assess the processing gains; we provide more details on them in section 3.3.

Although the chosen non-deep methods vary greatly in type and options from paper to paper, there are still numerous cases where DNNs are compared to an SVM-based implementation, with Random Forest and KNN being the next classifier types used by much less frequency in our observed cases. Therefore we chose those papers reporting on SVM results as the candidates for doing our quantitative analysis (in the next section). SVM is a good choice for benchmarking because it is a well-established and proven classification tool with generally superior performance (Mountrakis et al. (2011); Khatami et al. (2016); Heydari and Mountrakis (2018)). Note that in remote sensing image or scene classification tasks, we are generally interested in both feature generation and classification. Neural networks can do both automatically – and deep

299 networks put more stress on the feature extraction task – but SVM classifiers should be fed with
300 features already generated by another algorithm. The SVM implementation itself may vary
301 between processing the raw pixels data or some secondary handcrafted spectral/spatial features
302 derived from data. To ensure a more fair comparison we separated these two cases due to the
303 potential important impact of working with features instead of raw data. Clearly, there are many
304 variations and methods for handcrafting features and each paper may include a different set of
305 methods for comparison, so we could not go into their implementations detail and a detailed
306 comparison. Furthermore, SVM optimization methods varied (e.g. hyperparameters and kernel
307 choice), however we assumed (and it was also stressed in some papers) that after tuning the
308 authors reported their best SVM performance.

309 We should mention here that although our meta-analysis covers many different cases, each
310 case has almost a unique setting of the above parameters and therefore our analysis is naturally
311 limited in depth and statistical richness. Our objective was to study general trends and for the
312 first time in the literature offer a quantitative meta-analysis of DNNs in remote sensing
313 applications. Our quantitative analysis did not go into a detailed analysis of the effect of every
314 design option due to lack of data.

315

316 ## 3. RESULTS AND DISCUSSION

317

318 ### 3.1.Descriptive statistics

319 Table 2 provides information on case studies distribution by year, network type, spatial
320 resolution and input dimensionality. Note that some manuscripts may contain more than one
321 study, and spatial or input dimensionality information was not always available.

322

Table 2: Basic statistics of collected case studies

| *Year* | *2014* | *2015* | *2016* | *2017* | *2018* |
|---|---|---|---|---|---|
| Number of publications | 4 | 27 | 21 | 22 | 33 |

| *Network Type* | *CNN* | *DBN* | *SAE* |
|---|---|---|---|
| Number of cases | 150 | 9 | 25 |

| *Dataset spatial resolution* | *< 30cm* | *30cm ~ 3m* | *> 3m* |
|---|---|---|---|
| Number of cases | 23 | 88 | 48 |

| *Spectral and auxiliary bands* | *1-3* | *4-10* | *11-99* | *> 100* |
|---|---|---|---|---|
| Number of cases | 59 | 48 | 1 | 70 |

There is an increase in research papers on deep networks for remote sensing classification applications after 2014, continuing to date. CNN is the most commonly used network type, then SAE followed by DBN. Most of the datasets are either hyperspectral (>100 spectral channels) or less than 10 channels. Just one case study had spectral channels between 10 and 100. Hyperspectral dataset are of high spatial resolution (around 1m) so sit in the middle group of spatial resolution category. Very high resolution ones (<30cm) are mostly available in RGB with possibly adding Near-Infrared band and/or DSM data to it, with just one very recent case incorporating a drone-based six band experiment at spatial resolution of 4.7cm . More information on datasets will be given in the next section.

### 3.2. Datasets in the selected case studies

A wide variety of approximately 60 different datasets were used throughout the selected case studies. They included frequently used datasets along with datasets selected from public sources such as Google Earth, QuickBird, WorldView, Landsat archives and proprietary data sources. Cases that have been used more than twice in our review are listed in Table 3. The table includes

both scene and pixel classification applications as indicated in the last column, and the "labelled elements" column should be interpreted accordingly. Among them, the Brazilian Coffee, NWPU-RESISC45, RSSCN7, UC Merced, and WHU-RS19 have been used for scene classification while the others concentrated on pixel classification/image segmentation. It is important to note a significant limitation. While still being extensively used even in papers from 2018, some of the commonly used datasets are old and outdated: the major issue is their small size compared to datasets with millions of elements typically used in computer vision and other artificial intelligence studies. This issue has been partly addressed by some very high resolution datasets such as ISPRS Vaihingen and Potdam datasets, which became a standard test bench for newly arrived (mostly CNN-based) networks. Furthermore, hyperspectral cases are limited to a single scene and some datasets cover a very small geographic area, which limits the generalization ability of the obtained results. Again, there is a new dataset presented through IEEE GRSS contest in 2018 which consists of a relatively large area of 1.4km$^2$ covered by both very high resolution (5cm) RGB and high resolution (1m) multispectral data. However, none of our reviewed articles was based on this new dataset (Le Saux et al., 2018).

There is a still a need to create more large and rich datasets for remote sensing applications in different spatial and spectral resolutions. Preparing datasets for tackling temporal applications is another important issue, which is even more restricted than other applications. However, the decision to pick specific labels and the procedure for creating ground truth maps is very application-specific. Provision of auxiliary data (commonly DSM based on LiDAR) is also an important enhancement that is available in few datasets and should be encouraged.

366 Table 3: Specifications for most frequently used datasets
367

| *Dataset name* | *Sensor platform* | *Dataset size* | *Image size (pixels)* | *Labelled elements* | *Spatial res.* | *# of spectral and aux. channels* | *# of classes / classification task* |
|---|---|---|---|---|---|---|---|
| Brazilian coffee | SPOT | 50000 | 64x64 | 50000 scenes | | RG + NI | 3 class, but highly imbalanced / scene |
| Houston (2013 GRSS) | ITRES-CASI | 1 | 1905x349 | 15029 | 2.5 m | 144 + LiDAR | 15 class / pixel |
| Indian pines | AVIRIS | 1 | 145x145 | 10249 | 20 m | 220 | 16 class / pixel |
| ISPRS Potsdam | Aerial photo | 38 | 6000x6000 | 24 full images (of 38) | 5 cm | RGB + NI + DSM | 6 class / pixel |
| ISPRS Vaihingen | Aerial photo | 33 | circa 2500x2000 | 16 full images (of 33) | 9 cm | RG + NI + DSM | 6 class / pixel |
| KSC (Kennedy Space Center) | AVIRIS | 1 | 512x614 | 5211 | 18 m | 224 | 13 class / pixel |
| NWPU-RESISC45 | Google Earth images | 31500 | 256x256 | 31500 scenes | 0.2 m ~ 30 m | RGB | 45 class, 700 samples per class / scene |
| Pavia Center | ROSIS | 1 | 512x614 | 148152 | 1.3 m | 103 | 9 class / pixel |
| Pavia University | ROSIS | 1 | 610x340 | 42776 | 1.3 m | 103 | 9 class / pixel |
| RSSCN7 | Google Earth images | 2800 | 400x400 | 2800 scenes | | RGB | 7 class, 400 samples per class / scene |
| Salinas | AVIRIS | 1 | 512x217 | 5348 | 3.7 m | 224 | 16 class / pixel |
| UC Merced | USGS satellite imagery | 2100 | 256x256 | 2100 scenes | 1 ft | RGB | 21 class, 100 samples per class / scene |
| WHU-RS19 | Google Earth images | 950 | 600x600 | 950 scenes | 0.5 m | RGB | 19 class, 50 samples per class / scene |

368
369

370 3.3. Network design options

371 In terms of network optimization for deep networks the simplest way is to change the
372 network depth (number of layers) and width (neurons per layer). Additional modifications
373 include changes in the activation function, the type of classifier or the training strategy
374 (supervised/unsupervised). Looking beyond these fairly common adjustments, we present in
375 Table 3 a descriptive summary of the most important design innovations we encountered. The
376 table is organized to titles summarizing the main design point, followed by specific design ideas
377 in each section. The number of papers using each option is provided to suggest popularity. Some

design options are not exclusive to a specific network type (e.g. network mixing options), while others are only applicable to specific network types (e.g. fully convolutional network). The classification task type may also require special provisions. For example, in image segmentation the objects' boundary alignment is of primary concern, while in scene classification this is not important. This makes edge enhancement techniques more relevant to the former application than the latter. As each design idea is presented and tested in a unique setting with single or multiple choices of listed options on different datasets and compared with different non-deep rivals, comparison between different design ideas and quantitative analysis of their merit is not possible. However, we discuss general findings on design options below and our intent is that this table will act as a preliminary catalog and guide future research, either through gap analysis or through frequently-implemented method identification.

*Dense (fully connected) networks:* This CNN-type network is the de-facto network of choice for very high resolution classification and almost all of the image segmentation works – particularly experiments with ISPRS Potsdam and Vaihingen datasets. The competition in this field is extensive, and some of the most popular networks have been implemented in this category to win the ISPRS competition. It is always possible to run the entire network and classify the image pixel by pixel, but it means a huge redundancy in calculations and therefore a direct map-to-map conversion (which typically contains chain of downsampling and then upsampling) is preferred. Upsampling design is a hot topic and each paper tries to find a better way to do it. Edge enhancement and additional segmentation techniques have also been examined by different approaches to enhance the result (we will refer to it in another paragraph in this section).

400 *Multiscale capability options:* This issue is of a particular interest in CNN networks due to
401 the limited connectivity of their neurons to the previous layer, but other network types may also
402 use it when they use a sliding window mechanism in their input layer. In custom CNN networks
403 the multiscale filters with or without skip links (forwarding features/scores from one layer to
404 another non-adjacent layer) is a promising choice, but this option is not typically available for
405 pre-trained networks.

406 *Network mixing options:* There is a variety of practices for this option as listed by categories
407 in Table 4. The most frequent option is ensemble of different networks or using a parallel
408 network on different bands (especially when the additional input in form of DSM or LiDAR is
409 provided). Parallel 1-D (spectral) and 2-D (spatial) network is also found in some cases, but
410 other forms of spectral/spatial input combination are more frequent (we discuss it in a later
411 paragraph). As the use of pretrained networks becomes more common, parallel networks are the
412 natural way of overcoming the imported network input limitation to RGB channels.

413 *Training options:* Engineering the input data is the most frequent form of enhancing training
414 operations in deep networks, which is implemented in a variety of methods. The simplest case is
415 to crop, rotate and flip the input patches (basic data augmentation) or adding virtual samples to
416 the input data (particularly used for making input set more balanced). Recently, active learning
417 and interactive sample selection approaches are gaining more attention. There are other specially
418 designed algorithms used to enhance data quality, such as salient patch selection; or specialized
419 methods for calculating network parameters, such as calculation of neurons weights by clustering
420 or PCA decomposition instead of training.

421 *Multimodal processing:* Deep networks in remote sensing classification started with
422 processing spectral components but quickly evolved to process other dimensions of data as well.

Data processing in spatial context is now typical, especially with CNN, and joint spectral-spatial processing in 3-D convolutional filters is popular. Before that, other techniques such as averaging over spatial dimension or PCA compression of spectral dimension were common, but newer 3-D architectures has shown slightly better performance in our case studies. The newest trend in multimode processing is to incorporate sequence/temporal processing, for example by treating spectral component of hyperspectral imagery as a (correlated) sequence, or working on time-series of spectral-spatial data cubes.

*Other features:* In addition to the above, we identified numerous special algorithms and techniques throughout our survey that are organized in this section. In earlier studies we saw some cases of performance improvement by feeding network with handcrafted features, but it seems to be an obsolete idea now. Object-based classification, image segmentation, and additional MRF/CRF processing have been attractive research areas from the early days and still draw a lot of attention. Parallel to that, developing and applying newer and more complicated network modules (for example residual modules in CNN or LSTM in RNN) in RS applications are increasing trends. In the reviewed cases, newly emerging modules seem to have the upper hand at the expense of much larger and more complicated networks. The other options found are:

- CRF postprocessing of deep network predictions to delineate and enhance object edges.
- Initial segmentation and creation of superpixels to feed deep network.
- Merging of deep network predicted map and segmented or CRF/MRF generated map based on network prediction confidence.
- Other pre/post processing methods (e.g. GLCM/gabor filters).

There is no dominant method among the aforementioned techniques and new methods are continuously emerging.

Table 4: Network options and design innovations in collected papers

| **Option** | **Frequency** |
|---|---|
| *Making dense (full resolution) output options (for CNN):* | |
| Fully Convolutional Network (convolution and deconvolution) | 13 |
| No down-sampling | 1 |
| *Multiscale capability options:* | |
| Getting multiscale input | 10 |
| Using multiscale kernels (filters) | 7 |
| Skip links (forwarding features/scores from one layer to another non-adjacent layer) | 8 |
| *Network mixing options (fusion/aggregation method varies by case):* | |
| Parallel handcrafted features | 3 |
| Parallel 1-D and 2-D convolutional networks | 3 |
| Parallel networks on different band combinations or sensors | 9 |
| Cascaded networks | 3 |
| Parallel (Ensemble) of different deep networks | 10 |
| *Training options:* | |
| Salient patches selection to train/test network | 2 |
| Active learning or iterative feature selection (removing inferior features) | 4 |
| Data augmentation or adding virtual samples to the input data | 15 |
| Other specialized methods | 9 |
| *Multimodal processing:* | |
| 3-D processing modules | 7 |
| Spatial averaging/filtering over a neighborhood for spectral+spatial input generation | 2 |
| PCA dimensionality reduction and spectral+spatial input generation | 9 |
| Sequence data/temporal processing | 4 |
| Other specialized methods | 2 |
| *Other features:* | |
| Feeding network with handcrafted features (not raw data) | 4 |
| Optimizing input band selection with genetic algorithms | 1 |
| MRF/CRF processing or boundary detection | 7 |
| Denoising SAE implementation | 3 |
| Initial and/or final data/feature filtering or segmentation to enhance object discrimination | 12 |
| Sparse or other type of coding to create codebook after feature generation and classify the code | 4 |
| Emerging network modules (e.g. residual module, inception module, LSTM) | 10 |

### 3.4. DNN vs. SVM classification accuracy comparisons

This section focuses on classification accuracy comparisons between DNN and SVM methods. We focused on SVM comparisons since the majority of the manuscripts we reviewed selected SVM as their benchmark. The SVM choice over other methods (e.g. RF) is further supported by a previously conducted meta-analysis, where SVM was found to outperform other (non-deep) methods (Khatami et al, 2016). A detailed table summarizing each study is available in Appendix A. For a case study to be considered both methods were tested on the same dataset and results were reported in the form of average or overall accuracy.

Deep networks are usually designed to employ high volumes of available spectral and spatial data. However, in many of the selected cases of pixel classification, the authors compare DNNs to simple spectral processing by SVM or other non-deep rivals, thus providing an unfair advantage to DNNs as they also incorporate spatial information. Knowledge of feature generation details may not be a primary concern in deep networks as it is optimized automatically by the network, but finding the best method for feature generation to feed an SVM is not a straightforward task that often requires trial and error for each dataset. On the other hand, designing the best deep networks out of standard basic schemes is not a trivial issue and we see new designs continuously arising. To further inform readers in all figures in this section, we marked the cases with enhanced feature generation for non-deep classifier (SVM) with a black circle to separate them from cases using exclusively spectral information in their SVM implementation. Initial summary results are depicted in figure 1. Also as there were just two cases with SVM accuracy below 70%, we set our scale to start from that and omitted those two in display to reduce the congestion on the upper accuracy values in the provided figures.

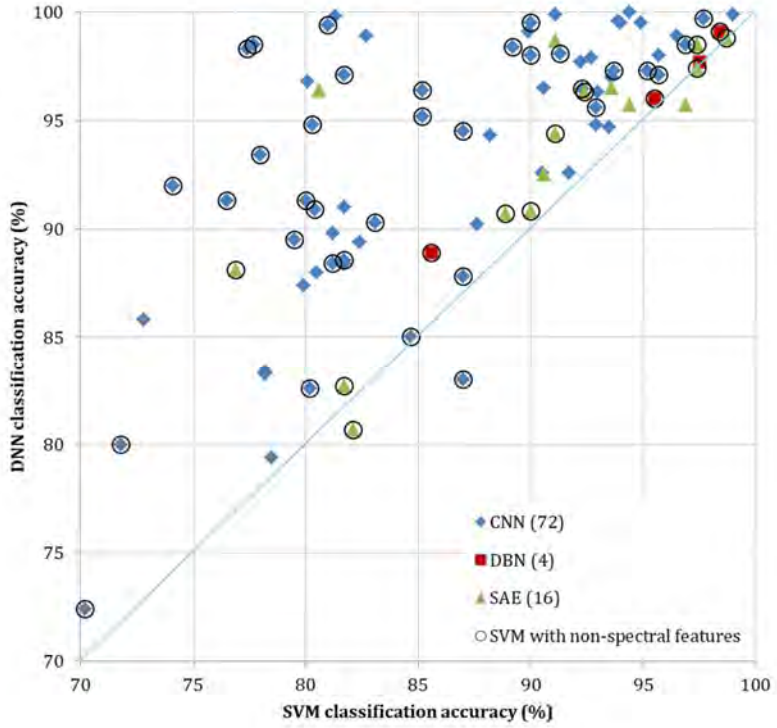


Figure 1: Comparative performance distribution of DNN vs SVM

In general, deep learning approaches offer consistently better results than SVM methods, even when only the cases with enhanced (non-spectral) features are considered. The reported improvement (difference in accuracy value) can be as high as 30% for CNN, 16% for SAE and 3% for DBN. The DBN values may not be very representative due to the scarcity of this network type application in remote sensing, but this lower application rate itself can be a sign of its lack of merit and/or underlying complexity. CNN accuracy benefits are often attributed to the integrated processing of spatial and spectral information, while for SAE or DBN benefits involve specific experimental design. As an example, one author used the average values of a neighborhood around each pixel (to be classified) for each band and added it to the central pixel's own data, then fed the SAE or DBN with this composite data vector. It is also common in hyperspectral image classification to process input image with dimensionality reduction

techniques such as PCA first, and then build the spatial information to be added to the original central pixel for classification.

CNN also has the ability to preserve the spatial relationships while processing through different layers, as spatial filtering takes place in each layer without flattening data to a row vector. In SAE or DBN implementations, the spatial information is flattened and concatenated to the spectral data at the network input, and although the spatial information is implicitly included, the spatial relations between vector values are lost (Y. Li et al. (2017); Yue et al. (2015); Basu et al. (2015)). However, the CNN spatial coverage is limited to a neighborhood of fixed size at the input, increasing step by step while resolution is reduced accordingly in pooling layers. This issue is restrictive to scale-dependent information, although it can be remedied to some extent by a multiscale structure (for example see X. Chen et al. (2014), Zhao et al. (2015), or Zhao and Du (2016)). Other networks are not inherently limited by these rules, though the strength of spatial relationships is generally reduced with the increasing distance from the central point according to Tobler's law in geography (Tobler (1970)). It is also important to consider that the SAE and DBN methods are trained in an unsupervised fashion while the CNN method follows a supervised approach. Therefore, the CNN implementation may be advantageous due to the incorporation of labeling information (Y. Li et al. (2017); Shi and Pun (2018)). SAE and DBN are also trained in a greedy layer-wise fashion that may limit potential learning opportunities; each layer's parameters are fixed when tuning the next layer. Joint training of layers for SAE and DBN has been proposed in Zhou et al. (2014) and reported to perform better than typical greedy layer-wise approach, but it is not of common use.

To investigate further DNN accuracy gains, we examined their distribution across five contributing factors, namely the DNN learning method, the network complexity, spatial

513 resolution, input dimensionality and training dataset proportion. Due to the low number of case
514 studies and variation of design parameters and datasets employed in different studies we do not
515 report a multivariable regression model. Instead, we limit our analysis to single factor
516 distribution plots.

517 *Distribution across learning methods.* Figures 2 and 3 present accuracy comparisons for
518 different learning methods for CNN and SAE, respectively. DBNs have a single learning option
519 therefore they are omitted from this analysis. Starting with Figure 2 and CNN methods, the
520 majority of cases have used supervised training or its enhanced version shown as supervised+
521 (cases with different cost function or optimization procedure, or being enhanced by data-driven
522 techniques such as active learning). CNNs using supervised learning is mostly compared to
523 spectral SVM and tend to offer higher relative gains in more complex classifications, where the
524 corresponding SVM accuracy is lower. This result is expected due to integration of spatial data
525 in CNN and lack of it in spectral SVM. As mentioned in Zhao et al. (2017), there are similarities
526 between low-level features in different classes that cannot be resolved solely by the spectral
527 components and integration of spatial data is required (an example is the road and building roof
528 pixels in an aerial image). As seen in the upper right corner of the graph, in cases where the
529 SVM was fed with enhanced features, the performance is fairly close to the supervised learning
530 DNN cases. One benefit of deep networks is the flexibility to build the features automatically
531 and match them to the specific dataset under study, contrary to handcrafted features that should
532 be selected among many variants for SVM or other non-deep classifiers.

533 Transfer learning in CNN also offers some improvements visible in Figure 2 – and especially
534 when combined with fine-tuning – over enhanced SVM. Base networks are typically taken from
535 models developed and trained in computer vision industry and will not be introduced here here.

The most widely used model in our reviewed cases as AlexNet (9 cases), followed by VGG-16 (8 cases), VGG-M (5 cases), and GoogLeNet (4 cases). Other networks have also been applied with lower frequency such as ResNet, other VGG-series networks, SegNet, Overfeat, and CaffeNet. Their improved performance over supervised learning CNN cases could be attributed to the fact that supervised CNN cases are usually custom designed and small in size compared to CNN networks used for transfer learning, therefore they may not be much more powerful than a SVM fed with enhanced features. A large fully supervised network may achieve considerable improvement over an enhanced SVM, but the computational budget might be prohibitive and the risk of overfitting high. Transfer learning, however, uses a proven network architecture that is pre-set using an extensive collection of labelled image data, and reduces user involvement into network design issues. Successful application of this technique suggests that the features generated by those large image collections have a good generalization capability and can be matched to arbitrary datasets assuming a fine-tuning step. Comparisons of different possibilities for feature extraction, supervised training and transfer learning (with or without fine tuning) for selected CNN architectures are described in detail in Nogueira et al. (2017) and tested for three well-known scene classification datasets. They suggest to use transfer learning and fine-tuning instead of fully supervised training because the pre-trained networks start from a better initialization state in the search space. A significant limitation though is that pre-trained networks are not currently applicable in multispectral/hyperspectral classification tasks because existing pre-trained networks come from computer vision - trained on ImageNet - using RGB images. However, as studied in Huang et al. (2018), we can mix a big pre-trained network fed by the RGB portion of spectrum with a smaller deep network capable of mining the entire spectrum and obtain good results. Such a combination can also be run on limited number of input samples as

559 the large network is pretrained. For the other options of semisupervised and unsupervised
560 learning we can see limited improvement but there are not enough samples for conclusive
561 results.

562

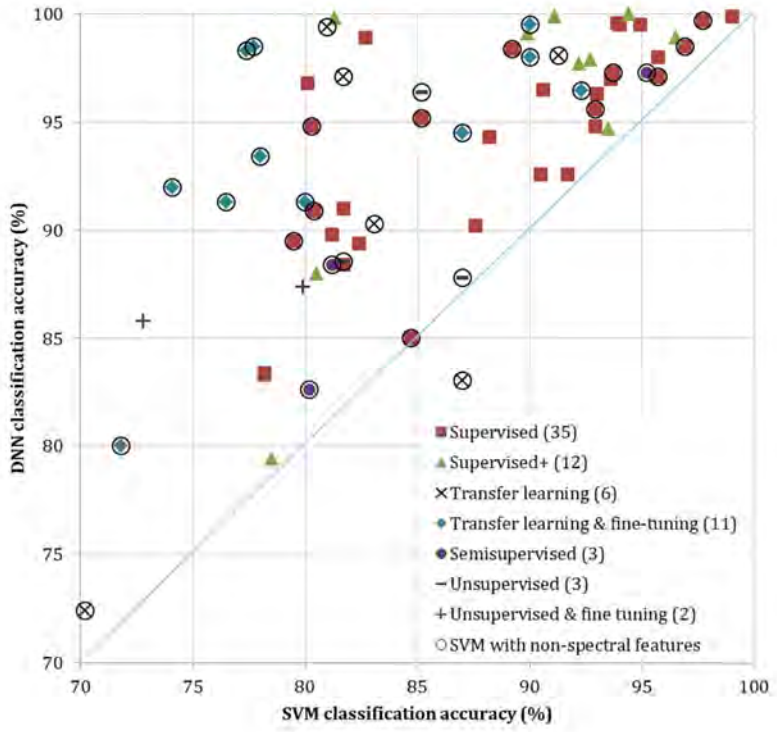


563
564
565 Figure 2: Comparative performance distribution across learning methods for CNN
566

567 Looking at figure 3 and the SAE learning methods, fine-tuning of unsupervised methods
568 tends to offer some gains over enhanced SVM, while there is no gain without fine-tuning. An
569 explanation could be that unsupervised learning receives its strength from using much more data
570 (labeled or unlabeled), so the features may be more representative of the data. However,
571 matching them to classes requires an extra step of supervised learning. Therefore, unsupervised
572 learning alone is comparable to enhanced SVM, and fine-tuning further improves results. Semi-
573 supervised learning was used in two cases with better results, but its application detail is case-

574 dependent. There are different methods and also underlying assumptions about actual class
575 distribution for doing semi-supervised learning (for example see Zhu and Goldberg (2009) and
576 Camps-Valls et al. (2014)). Each method and assumption is embedding a specific additional
577 regularization term for unlabeled data in the optimization cost function but there is no
578 standardized way of doing that. This lack of standardization may be a cause for its limited use.

579
580

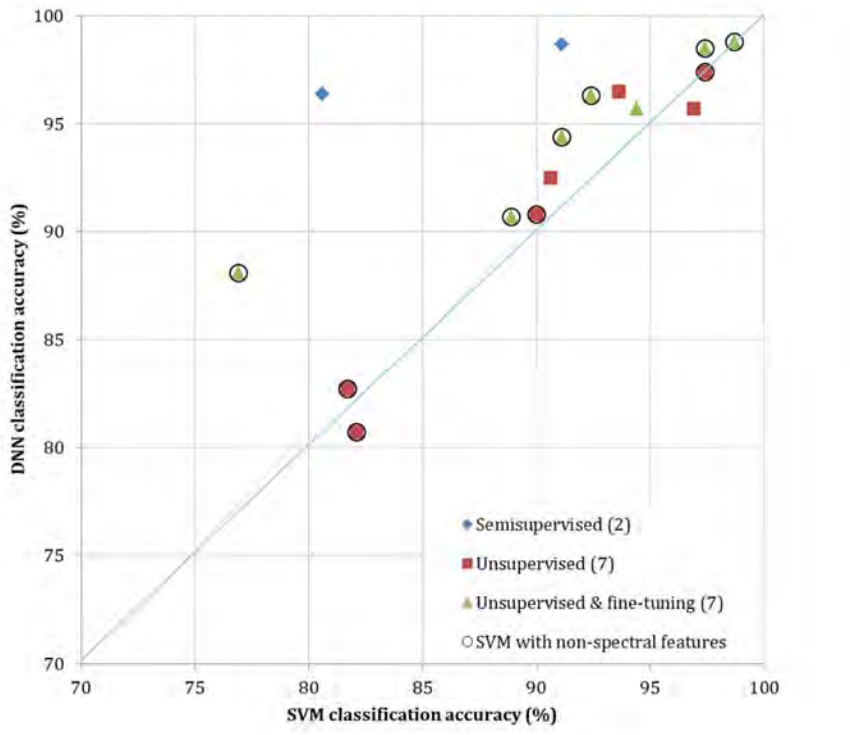


581
582 Figure 3: Comparative performance distribution across learning methods for SAE
583
584 *Distribution across network complexity.* To examine this, we discretized the number of
585 parameters to six bins from less than 10K (class A) to greater than 100M (class F); the result is
586 shown in Figure 4. Extremely low end (class A) cases are rare and do not seem to offer
587 considerable improvements. Class B has the highest frequency (23 cases), then class C, D, E, and
588 F with 16, 11, 10, and 9 cases correspondingly. It can be seen that class B, which is a still

relatively small network, has been compared to spectral SVM only and is mostly present in the upper right part of the graph, where the performance of spectral SVM is already high. These cases are those mostly associated with supervised learning method mentioned before. But larger networks (especially classes D and F) show considerable improvements over enhanced SVM. Based on this, we may advise to use larger networks (with fine-tuning) as mentioned before. However, this graph also demonstrates that all network complexity classes have the potential to achieve accuracy of 95% or more, which may be sufficient for many cases, especially considering other data limitations (e.g. registration errors). Note that class F cases are all ImageNet pre-trained networks, which are naturally the largest networks in our study cases.

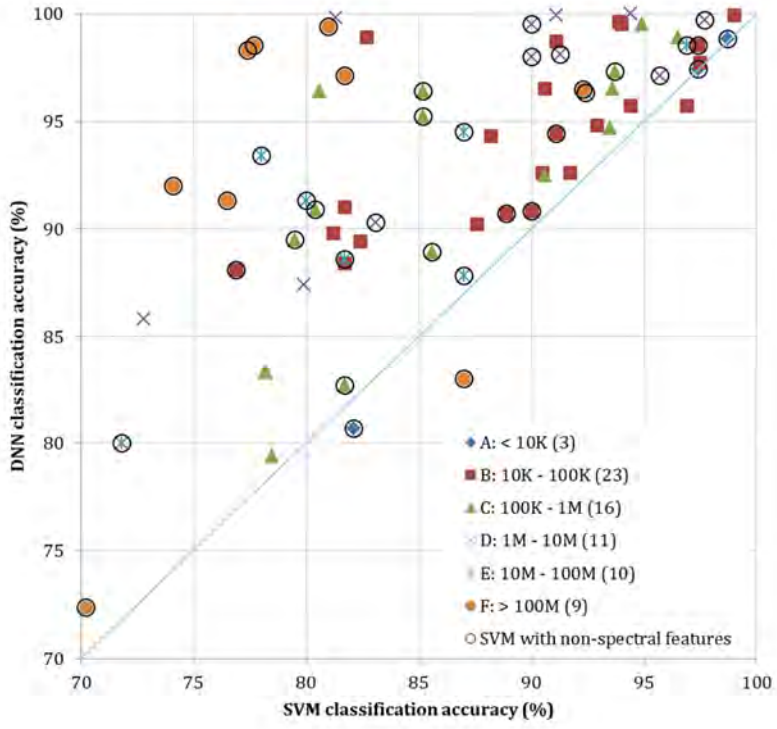


Figure 4: Comparative performance distribution across network complexity

*Distribution across spatial resolution.* The corresponding graph is shown in Figure 5. It is difficult to discern a specific pattern with respect to the spatial resolution, therefore no conclusive remarks could be made.

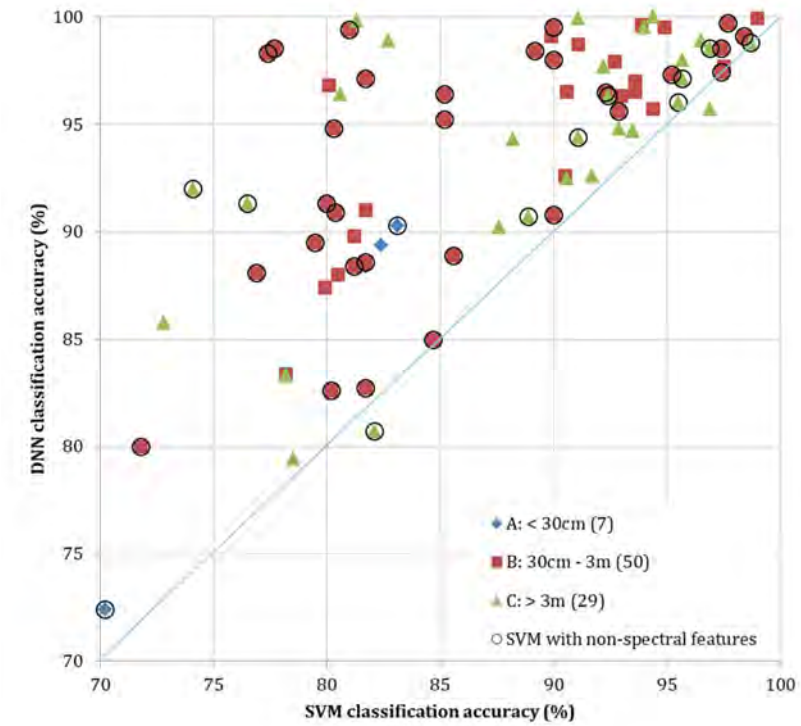


Figure 5: Comparative performance distribution across spatial resolution

*Distribution across input data dimensionality.* Figure 6 organizes the results in three general categories, mostly separating RGB (group A) and hyperspectral images (group C), with group B being cases employing additional multispectral components such as NI and/or auxiliary data such as DSM/LiDAR. Although it seems that multispectral group (B) generally achieves a bit less improvement compared to other two groups, there is no strong evidence and supporting theory for that.

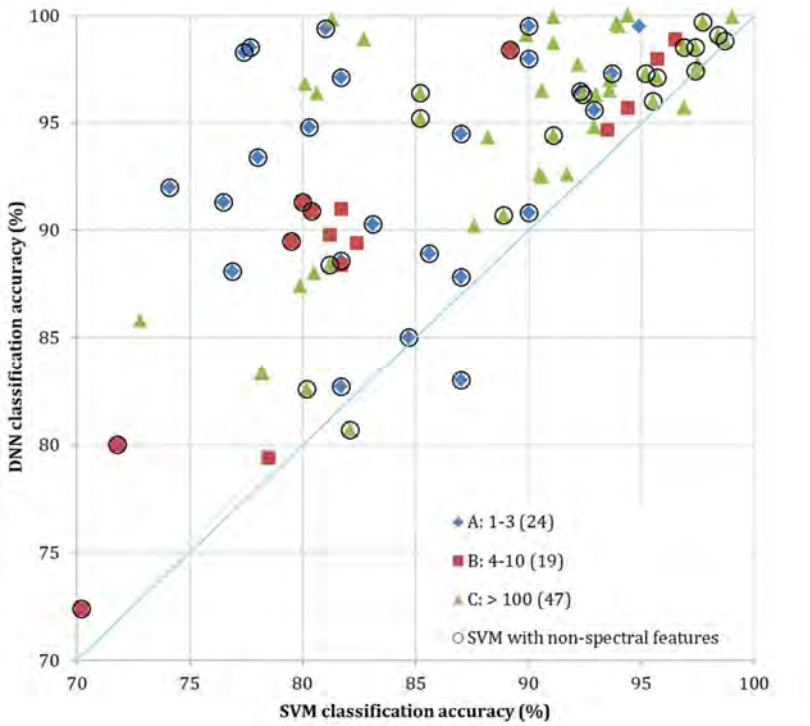


Figure 6: Comparative performance distribution across input data dimensionality

*Distribution across training size/proportion.* In the examined manuscripts the sampling is either a single pixel (for pixel classification or image segmentation applications) or an image patch (for scene classification or target detection applications). Labeled data size is mostly in the order of a few thousands, with additional cases with considerably more labelled data. Sampling is done within the labelled dataset, with the proportion varying substantially in different implementations from as low as 0.1% to as high as 90%. We consider two different ways of training data size affecting network simulations. The first issue is the training data size, which should be considered in accordance to the network size and number of parameters. A large network with few training data may experience overfitting and lack of generalization, while a small network may not be powerful enough to model a complex set of training data. The other issue is the training data proportion, which imposes the same underfitting/overfitting scenario.

We compared the absolute number of training data units (pixels or scenes) to the number of network parameters in our database and found that in almost 90% of cases we have less data units than networks parameters to be tuned. The overfitting control mechanisms such as regularization are always included in the network design and it will alleviate overfitting problem, but there is still a substantial difference between the remote sensing and computer vision fields, as we have very large reference datasets in the latter. Looking at Table 4, the only case with millions of samples in remote sensing are ISPRS datasets, but the winners are all CNNs and there is no comparison reported with SVMs (competition is just between different CNN architectures) so we couldn't include them in our SVM-based charts.

In order to examine how DNN gains are influenced by training data absolute size and relative proportion with respect to the testing data two figures were produced. Figure 7 shows the comparative performance categorized in training proportions from A (less than 20%) to E (greater than 80%), and figure 8 groups cases by absolute training dataset size from A (below 1000) to E (over one hundred thousand). The observed variability in the graphs and the lack of a consistent pattern suggest that high training size or proportion are not a general requirement for deep learning algorithms because there are various cases of high (> 95%) overall accuracy from very low to very high sampling ratio or size. A closer examination took place to further investigate training size and proportion with respect to network and learning method type. In cases of DBN, the training proportion was always high (> 50%) but there was no explanation or justification for it in the reviewed articles. In general, the CNN methods with supervised learning have been used in all training proportions, while CNNs with transfer learning with fine-tuning were run with higher training proportion. This may be attributed to overfitting concerns in transfer learning cases, as the base network is usually large with millions of parameters.

Therefore, it is an open question how the transfer learning works in remote sensing cases where low training ratios are predominant.

There is also another concern that has not been discussed in the reviewed papers. About 64% of the cases in our entire database (and about 73% of cases used in the figures) belong to pixel classification category with the rest focusing on scene classification. In scene classification cases we have completely separate train and test scenes, therefore adding spatial data in training phase (which naturally happens in any CNN network) will not affect the testing performance. In pixel classification application the train and test pixels are chosen independently, but if the spatial processing is part of algorithm (that is typical), the training and testing pixels' neighborhoods may overlap and this may violate the basic assumption of independent training/testing samples. The real impact of this issue is not discussed in any of reviewed literature and it seems that the authors didn't consider it critical. It can be also argued that with multiple pooling layers in a CNN network and enlarging scale of pixel influence, there is always some trace of even far pixels on training phase. Therefore, strictly enforcing independency rule to the neighboring pixels may invalidate all of the CNN networks, which is no desire for anybody.

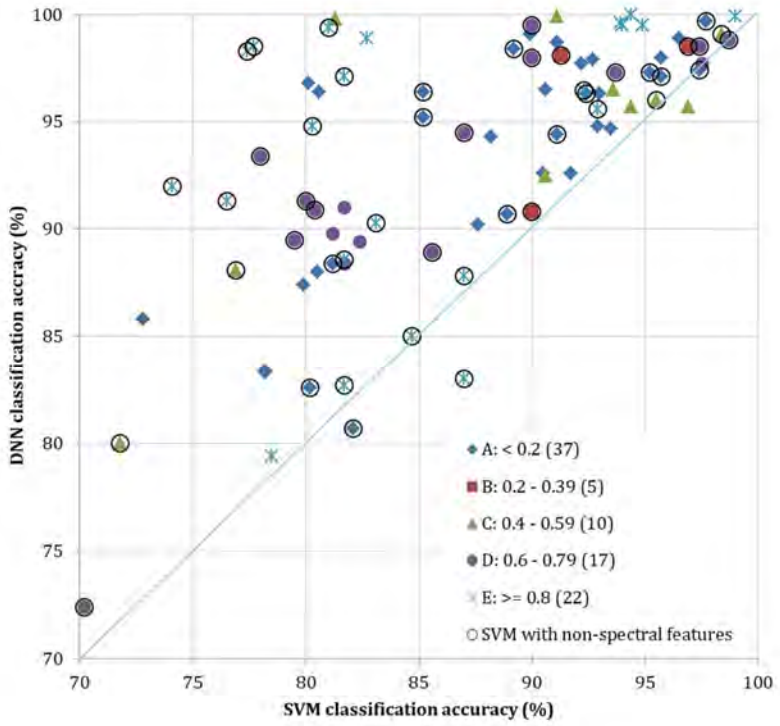


Figure 7: Comparative performance distribution across training proportion

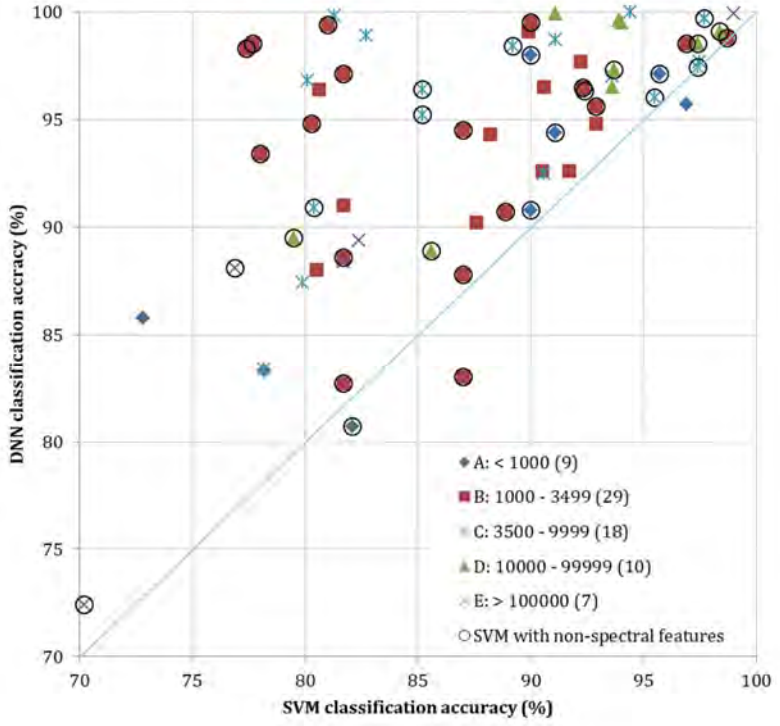

Figure 8: Comparative performance distribution across training data size

*Review of widely-used data sets.* In previous sections the objective was to reveal patterns (or lack of any pattern) in different networks comparative performance along important parameters. The main limitation of this analysis is that the comparisons could not be done by varying just one parameter and fixing the others while we could not have such a control in our data collection (hence we used the term 'distribution' instead of 'effect' in our section titles). In this section we go one step further and look at different cases as applied on the same dataset to extract more information on the competency of different network types. There are some datasets that are heavily used in various papers and therefore can serve as a benchmark for algorithmic comparison. Except for ISPRS Potsdam and ISPRS Vaihingen (where comparison to SVM was not available),figure 9 shows the result graphically.

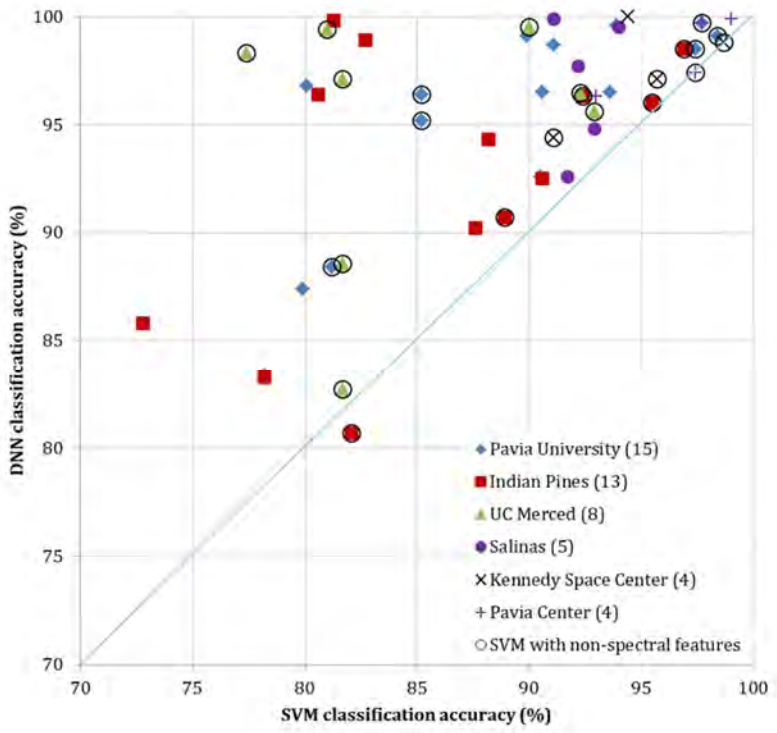

Figure 9: Comparative performance distribution across widely used datasets

Here are some observations:

- Indian Pines (a hyperspectral dataset): The highest accuracy here is obtained by CNN at 99.8% overall accuracy, but SAE and CNN have generally the same level of performance. Their improvement over spectral SVM can be as large as 16% for both network types. However, this high gain is reduced to just about 2-4% in comparison to enhanced SVM cases.
- Kennedy Space Center (a hyperspectral dataset): Recently CNN achieved an accuracy of 100% on this dataset (Haut et al., 2018) but with a high training proportion of 85% and 5.6% gain improvement over spectral SVM. Other comparisons were made with CNN and SAE but with enhanced SVM. The best accuracy of SAE was 98.8%, which was almost the same as a very sophisticated SVM implementation.
- Pavia Center (a hyperspectral dataset): CNN implementations show a little improvement up to 3.3% with training proportion of10%. The peak achieved accuracy was 99.95% but with a training proportion of 80% with very minor gains over SVM, and in all cases it was compared to the spectral SVM. We have only one SAE implementation for this dataset in our list, which does not improve over the enhanced SVM.
- Pavia University (a hyperspectral dataset): Here CNN here works better than SAE with a maximum overall accuracy of 99.7% and improvements up to 16.7% over spectral SVM, while for SAE it is at most 7.6% (both with training proportion of 10%).We have about 2% improvement over a very sophisticated SVM implementation for this dataset, but for SAE the gain over enhanced SVM is minor.

- Salinas (a hyperspectral dataset): This dataset was only applied to CNN and the best achieved accuracy was 99.9% with a training proportion of 50%. This was 8% gain in accuracy compared to spectral SVM, and other results showed some other gains. But there was no case of comparison with enhanced SVM.
- UC Merced (an RGB dataset used for scene classification): Here CNN works well with maximum overall accuracy of 99.5% and improvement up to 21% over SVM, while SAE was tested once with improvement of just 1%. In all cases, training proportion was high (60%-80%) and it was compared to enhanced SVM, but SVM was fed with very different features in different cases.

For the ISPRS Potsdam and Vaihingen datasets, the CNNs has been the winner over all of the recent contests, so the race is only between them and there is no research that compare them to a SVM based classification. Therefore, we could not include them in figure 7. In both ISPRS datasets the best results are achieved by transfer learning & fine-tuning in recent years. The best case was based on ResNet-101 with overall accuracy of 91.1% for both cases, followed by VGG-16 and SegNet-based cases with overall accuracy of 90.3%. Training proportion is standardized at 30% for Vaihingen and 45% for Potsdam (except ResNet-101 case, where the training proportion was 47% and 63%, respectively). These implementations are large networks, but a recent paper (Zhang et al., 2018b) has also achieved accuracies of 89.4% for Potsdam and 88.4% for Vaihingen with a small supervised network with number of parameters much less than above transferred networks (but with increasing training proportion to 70-75%). In almost all cases additional enhancement techniques such as joint segmentation, CRF processing or multiscale blocks has been implemented to boost the performance a bit higher.

744 The above datasets, while used extensively for classification assessment, should be avoided
745 in the future. They are relatively small to match the generalization capabilities of deep networks
746 and in most cases there are already algorithms that reach 100% accuracy, therefore offering
747 limited opportunities for improvement. It is necessary to develop new, large and multi-sensory
748 datasets for remote sensing image classification, especially for hyperspectral data, to help better
749 investigate the potential of deep networks.

750
751 ## 4. CONCLUDING REMARKS
752
753 While the number of case studies precluded detailed statistical analysis on the effect of each
754 contributing factors generally we can see that:

755 - Deep networks have generally better performance than spectral SVM implementations, with
756 CNNs performing better than other deep learners. This advantage, however, diminishes when
757 using SVM over more rich features extracted from data.
758 - Transfer learning and fine-tuning on pre-trained CNNs offer promising results even when
759 compared to enhanced SVM implementations, and they provide for flexibility and scalability
760 because there is no need to manually engineer the features or use a very large training
761 dataset. However, these pre-trained networks are currently limited to RGB input data,
762 therefore currently lack applicability in multi/hyperspectral data. They have also not been
763 tested in low training proportion scenarios.
764 - There is no strong relationship between network complexity and accuracy gains over SVM;
765 small to medium networks perform similarly to more complex networks.
766 - Contrary to popular belief, there are numerous cases of good deep network performance with
767 training proportions of 10% or lower.

As previously noted, deep networks are important due to their ability to extract useful rich features automatically from large data sets without the need for manual feature extraction. For example, automatic feature extraction has been used in Rußwurm and Körner (2018) to automatically detect cloud occlusion in temporal remote sensing data. This automation of feature extraction also has limitations, most notably the difficulty to extract and evaluate these features. The visualizations in deep networks rarely go further than the first two layers, which focus on very basic features like edges and gradients. There have been limited trials to describe and visualize the extracted features and even developing methods for it (for example see Zeiler and Fergus (2013) or Yosinski et al. (2015)), but currently research is lacking in remote sensing tasks.

We compare different studies and reflect on their findings in a collective manner. The possible reasons for deep network strengths in each individual aspect (network type, learning strategy, sampling proportion, etc.) was discussed in previous sections without going into mathematical formulas, due to the nature of meta-analysis. The majority of manuscripts reported that the SVM (or other rivals) parameters have been tuned and optimized for best performance, but there is a lack of consistency in reporting and protocol (e.g. grid search density). Establishing best optimization practices would benefit our community by limiting inconsistencies that could lead to result bias.

Another important conclusion is that algorithms are now outpacing benchmark datasets. We already see accuracy estimations exceeding 99% for some well-known datasets such as Indian Pine, Pavia Center and University, Salinas, and UC Merced. To allow deep learners to reach their full potential, it is paramount that more elaborate benchmark datasets should become available with diverse spectral/spatial/temporal resolution and geographic coverage.

We could not analyze further the processing time because either it was not available in many cases, or it was not specified if it contains the entire time for optimizing meta-parameters or not. It is generally true that deep networks need considerably more processing time for training (though the testing/simulation process is generally quick) but with continuous increases in processing power, deep networks are readily usable particularly by incorporating both CPUs and GPUs together.. It would be interesting to evaluate the time saved by using pre-trained networks and just fine-tuning them, but currently there were no statistics reported to extract conclusive guidance.

There are numerous design options currently offered (see Table 3). Multiscale input is particularly useful to capture geographic relationships in earth observations. Furthermore, fully convolutional networks are promising for dense semantic labeling (classification of all image pixels at once and producing the same output dense map as the input image size). Other researches have added various segmentation techniques, boundary detection and correction methods and CRF/MRF post-processing and showed their benefit to enhance classification of edge pixels. While existing comparisons suggest the potential of CNN, they do not concretely identify a winning design among different options. For example, at the ISPRS Vaihingen image segmentation contest three CNN methods were within 1.2% of overall accuracy (Sherrah (2016); Audebert et al. (2016); and Marmanis et al. (2016b)). Looking into the future, remote sensing experts will favor 3-D CNN structures from pre-processing, dimensionality reduction methods like PCA or shallow 1-D and 2-D networks. The current state of the art 3-D CNN structures has already offered significant improvements and the training process is becoming easier (see Chen et al. (2016) and Y. Li et al. (2017)). Furthermore, our community would significantly benefit from a coordinated investment from large funding institutions to create a pre-trained DNN for

814 remote sensing data (similar to the ImageNet for RBG images). This pre-trained network would
815 harness the power of large data volumes while allowing fine-tuning to specific applications.
816

817 ## 5. ACKNOWLEDGMENTS
818
819 This work was supported by the USDA McIntire Stennis program, a SUNY ESF Graduate
820 Assistantship and NASA's Land Cover Land Use Change Program (grant # NNX15AD42G).
821

## 6. REFERENCES


Aptoula, E., Ozdemir, M.C., Yanikoglu, B., 2016. Deep Learning With Attribute Profiles for Hyperspectral Image Classification. IEEE Geosci. Remote Sens. Lett. 13, 1970–1974. https://doi.org/10.1109/LGRS.2016.2619354

Audebert, N., Le Saux, B., Lefèvre, S., 2016. Semantic segmentation of earth observation data using multimodal and multi-scale deep networks, in: Asian Conference on Computer Vision. Springer, Cham, pp. 180–196.

Basaeed, E., Bhaskar, H., Al-Mualla, M., 2016. Supervised remote sensing image segmentation using boosted convolutional neural networks. Knowl.-Based Syst. 99, 19–27. https://doi.org/10.1016/j.knosys.2016.01.028

Basu, S., Ganguly, S., Mukhopadhyay, S., DiBiano, R., Karki, M., Nemani, R., 2015. Deepsat: a learning framework for satellite imagery, in: Proceedings of the 23rd SIGSPATIAL International Conference on Advances in Geographic Information Systems. ACM, p. 37.

Ben Hamida, A., Benoit, A., Lambert, P., Ben Amar, C., 2018. 3-D Deep Learning Approach for Remote Sensing Image Classification. IEEE Trans. Geosci. Remote Sens. 56, 4420–4434. https://doi.org/10.1109/TGRS.2018.2818945

Bengio, Y., 2009. Learning Deep Architectures for AI. Found. Trends Mach. Learn. 2, 1–127. https://doi.org/10.1561/2200000006

Bittner, K., Cui, S., Reinartz, P., 2017. Building extraction from remote sensing data using fully convolutional networks. ISPRS - Int. Arch. Photogramm. Remote Sens. Spat. Inf. Sci. XLII-1/W1, 481–486. https://doi.org/10.5194/isprs-archives-XLII-1-W1-481-2017

Camps-Valls, G., Tuia, D., Bruzzone, L., Benediktsson, J.A., 2014. Advances in Hyperspectral Image Classification: Earth Monitoring with Statistical Learning Methods. IEEE Signal Process. Mag. 31, 45–54. https://doi.org/10.1109/MSP.2013.2279179

Cao, Y., Niu, X., Dou, Y., 2016. Region-based convolutional neural networks for object detection in very high resolution remote sensing images. IEEE, pp. 548–554. https://doi.org/10.1109/FSKD.2016.7603232

Castelluccio, M., Poggi, G., Sansone, C., Verdoliva, L., 2015. Land Use Classification in Remote Sensing Images by Convolutional Neural Networks. ArXiv150800092 Cs.

Chen, F., Ren, R., Van de Voorde, T., Xu, W., Zhou, G., Zhou, Y., 2018. Fast Automatic Airport Detection in Remote Sensing Images Using Convolutional Neural Networks. Remote Sens. 10, 443. https://doi.org/10.3390/rs10030443

Chen, X., Xiang, S., Liu, C.-L., Pan, C.-H., 2014. Vehicle Detection in Satellite Images by Hybrid Deep Convolutional Neural Networks. IEEE Geosci. Remote Sens. Lett. 11, 1797–1801. https://doi.org/10.1109/LGRS.2014.2309695

Chen, X., Xiang, S., Liu, C.-L., Pan, C.-H., 2013. Aircraft Detection by Deep Belief Nets. IEEE, pp. 54–58. https://doi.org/10.1109/ACPR.2013.5

Chen, Y., Jiang, H., Li, C., Jia, X., Ghamisi, P., 2016. Deep Feature Extraction and Classification of Hyperspectral Images Based on Convolutional Neural Networks. IEEE Trans. Geosci. Remote Sens. 54, 6232–6251. https://doi.org/10.1109/TGRS.2016.2584107

Chen, Y., Lin, Z., Zhao, X., Wang, G., Gu, Y., 2014. Deep Learning-Based Classification of Hyperspectral Data. IEEE J. Sel. Top. Appl. Earth Obs. Remote Sens. 7, 2094–2107. https://doi.org/10.1109/JSTARS.2014.2329330

867 Chen, Y., Zhao, X., Jia, X., 2015. Spectral-Spatial Classification of Hyperspectral Data Based on
868 Deep Belief Network. IEEE J. Sel. Top. Appl. Earth Obs. Remote Sens. 8, 2381–2392.
869 https://doi.org/10.1109/JSTARS.2015.2388577
870 Cheng, G., Han, J., Lu, X., 2017a. Remote Sensing Image Scene Classification: Benchmark and
871 State of the Art. Proc. IEEE 105, 1865–1883.
872 https://doi.org/10.1109/JPROC.2017.2675998
873 Cheng, G., Li, Z., Yao, X., Guo, L., Wei, Z., 2017b. Remote Sensing Image Scene Classification
874 Using Bag of Convolutional Features. IEEE Geosci. Remote Sens. Lett. 14, 1735–1739.
875 https://doi.org/10.1109/LGRS.2017.2731997
876 Cui, W., Zheng, Z., Zhou, Q., Huang, J., Yuan, Y., 2018. Application of a parallel spectral–
877 spatial convolution neural network in object-oriented remote sensing land use
878 classification. Remote Sens. Lett. 9, 334–342.
879 https://doi.org/10.1080/2150704X.2017.1420265
880 Deng, L., 2014. A tutorial survey of architectures, algorithms, and applications for deep learning.
881 APSIPA Trans. Signal Inf. Process. 3. https://doi.org/10.1017/atsip.2013.9
882 Ding, C., Li, Y., Xia, Y., Wei, W., Zhang, L., Zhang, Y., 2017. Convolutional Neural Networks
883 Based Hyperspectral Image Classification Method with Adaptive Kernels. Remote Sens.
884 9, 618. https://doi.org/10.3390/rs9060618
885 Fu, G., Liu, C., Zhou, R., Sun, T., Zhang, Q., 2017. Classification for High Resolution Remote
886 Sensing Imagery Using a Fully Convolutional Network. Remote Sens. 9, 498.
887 https://doi.org/10.3390/rs9050498
888 Geng, J., Fan, J., Wang, H., Ma, X., Li, B., Chen, F., 2015. High-Resolution SAR Image
889 Classification via Deep Convolutional Autoencoders. IEEE Geosci. Remote Sens. Lett.
890 12, 2351–2355. https://doi.org/10.1109/LGRS.2015.2478256
891 Ghamisi, P., Chen, Y., Zhu, X.X., 2016. A Self-Improving Convolution Neural Network for the
892 Classification of Hyperspectral Data. IEEE Geosci. Remote Sens. Lett. 13, 1537–1541.
893 https://doi.org/10.1109/LGRS.2016.2595108
894 Ghamisi, P., Plaza, J., Chen, Y., Li, J., Plaza, A.J., 2017. Advanced Spectral Classifiers for
895 Hyperspectral Images: A review. IEEE Geosci. Remote Sens. Mag. 5, 8–32.
896 https://doi.org/10.1109/MGRS.2016.2616418
897 Gong, M., Zhan, T., Zhang, P., Miao, Q., 2017. Superpixel-Based Difference Representation
898 Learning for Change Detection in Multispectral Remote Sensing Images. IEEE Trans.
899 Geosci. Remote Sens. 55, 2658–2673. https://doi.org/10.1109/TGRS.2017.2650198
900 Gong, X., Xie, Z., Liu, Y., Shi, X., Zheng, Z., 2018. Deep Salient Feature Based Anti-Noise
901 Transfer Network for Scene Classification of Remote Sensing Imagery. Remote Sens. 10,
902 410. https://doi.org/10.3390/rs10030410
903 Goodfellow, I., Bengio, Y., Courville, A., 2016. Deep Learning. The MIT Press, Cambridge,
904 Massachusetts.
905 Gu, X., Angelov, P.P., Zhang, C., Atkinson, P.M., 2018. A Massively Parallel Deep Rule-Based
906 Ensemble Classifier for Remote Sensing Scenes. IEEE Geosci. Remote Sens. Lett. 15,
907 345–349. https://doi.org/10.1109/LGRS.2017.2787421
908 Han, W., Feng, R., Wang, L., Cheng, Y., 2018. A semi-supervised generative framework with
909 deep learning features for high-resolution remote sensing image scene classification.
910 ISPRS J. Photogramm. Remote Sens. 145, 23–43.
911 https://doi.org/10.1016/j.isprsjprs.2017.11.004

912 Haut, J.M., Paoletti, M.E., Plaza, J., Li, J., Plaza, A., 2018. Active Learning With Convolutional
913 Neural Networks for Hyperspectral Image Classification Using a New Bayesian
914 Approach. IEEE Trans. Geosci. Remote Sens. 56, 6440–6461.
915 https://doi.org/10.1109/TGRS.2018.2838665
916 Heydari, S.S., Mountrakis, G., 2018. Effect of classifier selection, reference sample size,
917 reference class distribution and scene heterogeneity in per-pixel classification accuracy
918 using 26 Landsat sites. Remote Sens. Environ. 204, 648–658.
919 https://doi.org/10.1016/j.rse.2017.09.035
920 Hinton, G.E., Osindero, S., Teh, Y.-W., 2006. A fast learning algorithm for deep belief nets.
921 Neural Comput. 18, 1527–1554. https://doi.org/10.1162/neco.2006.18.7.1527
922 Hu, F., Xia, G.-S., Hu, J., Zhang, L., 2015. Transferring Deep Convolutional Neural Networks
923 for the Scene Classification of High-Resolution Remote Sensing Imagery. Remote Sens.
924 7, 14680–14707. https://doi.org/10.3390/rs71114680
925 Hu, J., Mou, L., Schmitt, A., Zhu, X.X., 2017. FusioNet: A two-stream convolutional neural
926 network for urban scene classification using PolSAR and hyperspectral data. IEEE, pp.
927 1–4. https://doi.org/10.1109/JURSE.2017.7924565
928 Hu, W., Huang, Y., Wei, L., Zhang, F., Li, H., 2015. Deep Convolutional Neural Networks for
929 Hyperspectral Image Classification. J. Sens. 2015, 1–12.
930 https://doi.org/10.1155/2015/258619
931 Huang, B., Zhao, B., Song, Y., 2018. Urban land-use mapping using a deep convolutional neural
932 network with high spatial resolution multispectral remote sensing imagery. Remote Sens.
933 Environ. 214, 73–86. https://doi.org/10.1016/j.rse.2018.04.050
934 Ishii, T., Nakamura, R., Nakada, H., Mochizuki, Y., Ishikawa, H., 2015. Surface object
935 recognition with CNN and SVM in Landsat 8 images. IEEE, pp. 341–344.
936 https://doi.org/10.1109/MVA.2015.7153200
937 Ji, S., Zhang, C., Xu, A., Shi, Y., Duan, Y., 2018. 3D Convolutional Neural Networks for Crop
938 Classification with Multi-Temporal Remote Sensing Images. Remote Sens. 10, 75.
939 https://doi.org/10.3390/rs10010075
940 Karalas, K., Tsagkatakis, G., Zervakis, M., Tsakalides, P., 2015. Deep learning for multi-label
941 land cover classification, in: Bruzzone, L. (Ed.), . p. 96430Q.
942 https://doi.org/10.1117/12.2195082
943 Kemker, R., Salvaggio, C., Kanan, C., 2018. Algorithms for semantic segmentation of
944 multispectral remote sensing imagery using deep learning. ISPRS J. Photogramm.
945 Remote Sens. 145, 60–77. https://doi.org/10.1016/j.isprsjprs.2018.04.014
946 Khan, S.H., He, X., Porikli, F., Bennamoun, M., 2017. Forest Change Detection in Incomplete
947 Satellite Images With Deep Neural Networks. IEEE Trans. Geosci. Remote Sens. 1–17.
948 https://doi.org/10.1109/TGRS.2017.2707528
949 Khatami, R., Mountrakis, G., Stehman, S.V., 2016. A meta-analysis of remote sensing research
950 on supervised pixel-based land-cover image classification processes: General guidelines
951 for practitioners and future research. Remote Sens. Environ. 177, 89–100.
952 https://doi.org/10.1016/j.rse.2016.02.028
953 Lagrange, A., Le Saux, B., Beaupere, A., Boulch, A., Chan-Hon-Tong, A., Herbin, S.,
954 Randrianarivo, H., Ferecatu, M., 2015. Benchmarking classification of Earth-observation
955 data: from learning explicit features to convolutional networks, in: IGARSS 2015.

Längkvist, M., Kiselev, A., Alirezaie, M., Loutfi, A., 2016. Classification and Segmentation of Satellite Orthoimagery Using Convolutional Neural Networks. Remote Sens. 8, 329. https://doi.org/10.3390/rs8040329

Le, Q.V., 2015. A Tutorial on Deep Learning Part 2: Autoencoders, Convolutional Neural Networks and Recurrent Neural Networks.

Le Saux, B., Yokoya, N., Hansch, R., Prasad, S., 2018. Advanced Multisource Optical Remote Sensing for Urban Land Use and Land Cover Classification [Technical Committees]. IEEE Geosci. Remote Sens. Mag. 6, 85–89. https://doi.org/10.1109/MGRS.2018.2874328

Lguensat, R., Sun, M., Fablet, R., Mason, E., Tandeo, P., Chen, G., 2017. EddyNet: A Deep Neural Network For Pixel-Wise Classification of Oceanic Eddies. ArXiv171103954 Phys.

Li, J., Bruzzone, L., Liu, S., 2015. Deep feature representation for hyperspectral image classification. IEEE, pp. 4951–4954. https://doi.org/10.1109/IGARSS.2015.7326943

Li, T., Zhang, J., Zhang, Y., 2014. Classification of hyperspectral image based on deep belief networks, in: 2014 IEEE International Conference on Image Processing (ICIP). Presented at the 2014 IEEE International Conference on Image Processing (ICIP), pp. 5132–5136. https://doi.org/10.1109/ICIP.2014.7026039

Li, W., Wu, G., Zhang, F., Du, Q., 2017. Hyperspectral Image Classification Using Deep Pixel-Pair Features. IEEE Trans. Geosci. Remote Sens. 55, 844–853. https://doi.org/10.1109/TGRS.2016.2616355

Li, Y., Zhang, H., Shen, Q., 2017. Spectral–Spatial Classification of Hyperspectral Imagery with 3D Convolutional Neural Network. Remote Sens. 9, 67. https://doi.org/10.3390/rs9010067

Liu, P., Choo, K.-K.R., Wang, L., Huang, F., 2017. SVM or deep learning? A comparative study on remote sensing image classification. Soft Comput. 21, 7053–7065. https://doi.org/10.1007/s00500-016-2247-2

Liu, S., Li, M., Zhang, Z., Xiao, B., Cao, X., 2018. Multimodal Ground-Based Cloud Classification Using Joint Fusion Convolutional Neural Network. Remote Sens. 10, 822. https://doi.org/10.3390/rs10060822

Liu, W., Wang, Z., Liu, X., Zeng, N., Liu, Y., Alsaadi, F.E., 2017. A survey of deep neural network architectures and their applications. Neurocomputing 234, 11–26. https://doi.org/10.1016/j.neucom.2016.12.038

Liu, Yongcheng, Fan, B., Wang, L., Bai, J., Xiang, S., Pan, C., 2018. Semantic labeling in very high resolution images via a self-cascaded convolutional neural network. ISPRS J. Photogramm. Remote Sens. 145, 78–95. https://doi.org/10.1016/j.isprsjprs.2017.12.007

Liu, Yanfei, Zhong, Y., Fei, F., Zhu, Q., Qin, Q., 2018. Scene Classification Based on a Deep Random-Scale Stretched Convolutional Neural Network. Remote Sens. 10, 444. https://doi.org/10.3390/rs10030444

Luus, F.P.S., Salmon, B.P., Bergh, F. van den, Maharaj, B.T.J., 2015. Multiview Deep Learning for Land-Use Classification. IEEE Geosci. Remote Sens. Lett. 12, 2448–2452. https://doi.org/10.1109/LGRS.2015.2483680

Lyu, H., Lu, H., Mou, L., 2016. Learning a Transferable Change Rule from a Recurrent Neural Network for Land Cover Change Detection. Remote Sens. 8, 506. https://doi.org/10.3390/rs8060506

Ma, L., Li, M., Ma, X., Cheng, L., Du, P., Liu, Y., 2017. A review of supervised object-based land-cover image classification. ISPRS J. Photogramm. Remote Sens. 130, 277–293. https://doi.org/10.1016/j.isprsjprs.2017.06.001

Ma, X., Geng, J., Wang, H., 2015. Hyperspectral image classification via contextual deep learning. EURASIP J. Image Video Process. 2015. https://doi.org/10.1186/s13640-015-0071-8

Ma, Z., Wang, Z., Liu, C., Liu, X., 2016. Satellite Imagery Classification Based on Deep Convolution Network. World Acad. Sci. Eng. Technol. 10.

Maggiori, E., Tarabalka, Y., Charpiat, G., Alliez, P., 2017. Convolutional Neural Networks for Large-Scale Remote-Sensing Image Classification. IEEE Trans. Geosci. Remote Sens. 55, 645–657. https://doi.org/10.1109/TGRS.2016.2612821

Maggiori, E., Tarabalka, Y., Charpiat, G., Alliez, P., 2016. High-Resolution Semantic Labeling with Convolutional Neural Networks. ArXiv Prepr. ArXiv161101962.

Makantasis, K., Karantzalos, K., Doulamis, A., Doulamis, N., 2015. Deep supervised learning for hyperspectral data classification through convolutional neural networks, in: Geoscience and Remote Sensing Symposium (IGARSS), 2015 IEEE International. IEEE, pp. 4959–4962.

Marcos, D., Volpi, M., Kellenberger, B., Tuia, D., 2018. Land cover mapping at very high resolution with rotation equivariant CNNs: Towards small yet accurate models. ISPRS J. Photogramm. Remote Sens. 145, 96–107. https://doi.org/10.1016/j.isprsjprs.2018.01.021

Marmanis, D., Datcu, M., Esch, T., Stilla, U., 2016a. Deep Learning Earth Observation Classification Using ImageNet Pretrained Networks. IEEE Geosci. Remote Sens. Lett. 13, 105–109. https://doi.org/10.1109/LGRS.2015.2499239

Marmanis, D., Schindler, K., Wegner, J.D., Galliani, S., Datcu, M., Stilla, U., 2016b. Classification with an edge: improving semantic image segmentation with boundary detection. ArXiv Prepr. ArXiv161201337.

Mou, L., Bruzzone, L., Zhu, X.X., 2018a. Learning Spectral-Spatial-Temporal Features via a Recurrent Convolutional Neural Network for Change Detection in Multispectral Imagery. ArXiv180302642 Cs.

Mou, L., Ghamisi, P., Zhu, X.X., 2018b. Unsupervised Spectral–Spatial Feature Learning via Deep Residual Conv–Deconv Network for Hyperspectral Image Classification. IEEE Trans. Geosci. Remote Sens. 56, 391–406. https://doi.org/10.1109/TGRS.2017.2748160

Mou, L., Ghamisi, P., Zhu, X.X., 2017. Deep Recurrent Neural Networks for Hyperspectral Image Classification. IEEE Trans. Geosci. Remote Sens. 55, 3639–3655. https://doi.org/10.1109/TGRS.2016.2636241

Mountrakis, G., Im, J., Ogole, C., 2011. Support vector machines in remote sensing: A review. ISPRS J. Photogramm. Remote Sens. 66, 247–259. https://doi.org/10.1016/j.isprsjprs.2010.11.001

Ndikumana, E., Ho Tong Minh, D., Baghdadi, N., Courault, D., Hossard, L., 2018. Deep Recurrent Neural Network for Agricultural Classification using multitemporal SAR Sentinel-1 for Camargue, France. Remote Sens. 10, 1217. https://doi.org/10.3390/rs10081217

Niculescu, S., Ienco, D., Hanganu, J., 2018. APPLICATION OF DEEP LEARNING OF MULTI-TEMPORAL SENTINEL-1 IMAGES FOR THE CLASSIFICATION OF COASTAL VEGETATION ZONE OF THE DANUBE DELTA. ISPRS - Int. Arch.

Photogramm. Remote Sens. Spat. Inf. Sci. XLII–3, 1311–1318. https://doi.org/10.5194/isprs-archives-XLII-3-1311-2018

Nogueira, K., Penatti, O.A.B., Santos, J.A. dos, 2017. Towards Better Exploiting Convolutional Neural Networks for Remote Sensing Scene Classification. Pattern Recognit. 61, 539–556. https://doi.org/10.1016/j.patcog.2016.07.001

Paisitkriangkrai, S., Sherrah, J., Janney, P., Hengel, A.V.-D., 2015. Effective semantic pixel labelling with convolutional networks and Conditional Random Fields, in: 2015 IEEE Conference on Computer Vision and Pattern Recognition Workshops (CVPRW). Presented at the 2015 IEEE Conference on Computer Vision and Pattern Recognition Workshops (CVPRW), pp. 36–43. https://doi.org/10.1109/CVPRW.2015.7301381

Pan, B., Shi, Z., Xu, X., 2018. MugNet: Deep learning for hyperspectral image classification using limited samples. ISPRS J. Photogramm. Remote Sens. 145, 108–119. https://doi.org/10.1016/j.isprsjprs.2017.11.003

Paoletti, M.E., Haut, J.M., Plaza, J., Plaza, A., 2018. A new deep convolutional neural network for fast hyperspectral image classification. ISPRS J. Photogramm. Remote Sens. 145, 120–147. https://doi.org/10.1016/j.isprsjprs.2017.11.021

Penatti, O.A.B., Nogueira, K., Santos, J.A. dos, 2015. Do deep features generalize from everyday objects to remote sensing and aerial scenes domains?, in: 2015 IEEE Conference on Computer Vision and Pattern Recognition Workshops (CVPRW). Presented at the 2015 IEEE Conference on Computer Vision and Pattern Recognition Workshops (CVPRW), pp. 44–51. https://doi.org/10.1109/CVPRW.2015.7301382

Qayyum, A., Malik, A.S., Saad, N.M., Iqbal, M., Faris Abdullah, M., Rasheed, W., Rashid Abdullah, T.A., Bin Jafaar, M.Y., 2017. Scene classification for aerial images based on CNN using sparse coding technique. Int. J. Remote Sens. 38, 2662–2685. https://doi.org/10.1080/01431161.2017.1296206

Rezaee, M., Mahdianpari, M., Zhang, Y., Salehi, B., 2018. Deep Convolutional Neural Network for Complex Wetland Classification Using Optical Remote Sensing Imagery. IEEE J. Sel. Top. Appl. Earth Obs. Remote Sens. 11, 3030–3039. https://doi.org/10.1109/JSTARS.2018.2846178

Romero, A., Gatta, C., Camps-Valls, G., 2016. Unsupervised Deep Feature Extraction for Remote Sensing Image Classification. IEEE Trans. Geosci. Remote Sens. 54, 1349–1362. https://doi.org/10.1109/TGRS.2015.2478379

Rosenblatt, F., 1958. The perceptron: A probabilistic model for information storage and organization in the brain. Psychol. Rev. 65, 386–408. https://doi.org/10.1037/h0042519

Rumelhart, D.E., Hinton, G.E., Williams, R.J., 1986. Learning representations by back-propagating errors. Nature 323, 533–536. https://doi.org/10.1038/323533a0

Rußwurm, M., Körner, M., 2018. Multi-Temporal Land Cover Classification with Sequential Recurrent Encoders. ArXiv180202080 Cs.

Rußwurm, M., Körner, M., 2017. Multi-Temporal Land Cover Classification With Long Short-Term Memory Neural Networks. ISPRS - Int. Arch. Photogramm. Remote Sens. Spat. Inf. Sci. XLII-1/W1, 551–558. https://doi.org/10.5194/isprs-archives-XLII-1-W1-551-2017

Sharma, A., Liu, X., Yang, X., 2018. Land cover classification from multi-temporal, multi-spectral remotely sensed imagery using patch-based recurrent neural networks. Neural Netw. 105, 346–355. https://doi.org/10.1016/j.neunet.2018.05.019

Sherrah, J., 2016. Fully convolutional networks for dense semantic labelling of high-resolution aerial imagery. ArXiv Prepr. ArXiv160602585.

Shi, C., Pun, C.-M., 2018. Superpixel-based 3D deep neural networks for hyperspectral image classification. Pattern Recognit. 74, 600–616. https://doi.org/10.1016/j.patcog.2017.09.007

Singhal, V., Gogna, A., Majumdar, A., 2016. Deep Dictionary Learning vs Deep Belief Network vs Stacked Autoencoder: An Empirical Analysis, in: Hirose, A., Ozawa, S., Doya, K., Ikeda, K., Lee, M., Liu, D. (Eds.), Neural Information Processing. Springer International Publishing, Cham, pp. 337–344. https://doi.org/10.1007/978-3-319-46681-1_41

Sun, X., Zhou, F., Dong, J., Gao, F., Mu, Q., Wang, X., 2017. Encoding Spectral and Spatial Context Information for Hyperspectral Image Classification. IEEE Geosci. Remote Sens. Lett. 14, 2250–2254. https://doi.org/10.1109/LGRS.2017.2759168

Tang, T., Zhou, S., Deng, Z., Zou, H., Lei, L., 2017. Vehicle Detection in Aerial Images Based on Region Convolutional Neural Networks and Hard Negative Example Mining. Sensors 17, 336. https://doi.org/10.3390/s17020336

Tao, C., Pan, H., Li, Y., Zou, Z., 2015. Unsupervised Spectral–Spatial Feature Learning With Stacked Sparse Autoencoder for Hyperspectral Imagery Classification. IEEE Geosci. Remote Sens. Lett. 12, 2438–2442. https://doi.org/10.1109/LGRS.2015.2482520

Tao, Y., Xu, M., Lu, Z., Zhong, Y., 2018. DenseNet-Based Depth-Width Double Reinforced Deep Learning Neural Network for High-Resolution Remote Sensing Image Per-Pixel Classification. Remote Sens. 10, 779. https://doi.org/10.3390/rs10050779

Tobler, W.R., 1970. A Computer Movie Simulating Urban Growth in the Detroit Region. Econ. Geogr. 46, 234. https://doi.org/10.2307/143141

Tschannen, M., Cavigelli, L., Mentzer, F., Wiatowski, T., Benini, L., 2016. Deep Structured Features for Semantic Segmentation. ArXiv160907916 Cs.

Vakalopoulou, M., Karantzalos, K., Komodakis, N., Paragios, N., 2015. Building detection in very high resolution multispectral data with deep learning features. IEEE, pp. 1873–1876. https://doi.org/10.1109/IGARSS.2015.7326158

Vincent, P., Larochelle, H., Lajoie, I., Bengio, Y., Manzagol, P.-A., 2010. Stacked Denoising Autoencoders: Learning Useful Representations in a Deep Network with a Local Denoising Criterion. J Mach Learn Res 11, 3371–3408.

Volpi, M., Tuia, D., 2017. Dense semantic labeling of subdecimeter resolution images with convolutional neural networks. IEEE Trans. Geosci. Remote Sens. 55, 881–893.

Wang, J., Song, J., Chen, M., Yang, Z., 2015. Road network extraction: a neural-dynamic framework based on deep learning and a finite state machine. Int. J. Remote Sens. 36, 3144–3169. https://doi.org/10.1080/01431161.2015.1054049

Wang, S.-H., Sun, J., Phillips, P., Zhao, G., Zhang, Y.-D., 2018. Polarimetric synthetic aperture radar image segmentation by convolutional neural network using graphical processing units. J. Real-Time Image Process. 15, 631–642. https://doi.org/10.1007/s11554-017-0717-0

Weng, Q., Mao, Z., Lin, J., Guo, W., 2017. Land-Use Classification via Extreme Learning Classifier Based on Deep Convolutional Features. IEEE Geosci. Remote Sens. Lett. 14, 704–708. https://doi.org/10.1109/LGRS.2017.2672643

Weng, Q., Mao, Z., Lin, J., Liao, X., 2018. Land-use scene classification based on a CNN using a constrained extreme learning machine. Int. J. Remote Sens. 39, 6281–6299. https://doi.org/10.1080/01431161.2018.1458346

Wu, H., Liu, B., Su, W., Zhang, W., Sun, J., 2016. Deep Filter Banks for Land-Use Scene Classification. IEEE Geosci. Remote Sens. Lett. 13, 1895–1899. https://doi.org/10.1109/LGRS.2016.2616440

Wu, H., Prasad, S., 2018. Semi-Supervised Deep Learning Using Pseudo Labels for Hyperspectral Image Classification. IEEE Trans. Image Process. 27, 1259–1270. https://doi.org/10.1109/TIP.2017.2772836

Xia, G.-S., Hu, J., Hu, F., Shi, B., Bai, X., Zhong, Y., Zhang, L., Lu, X., 2017. AID: A Benchmark Data Set for Performance Evaluation of Aerial Scene Classification. IEEE Trans. Geosci. Remote Sens. 55, 3965–3981. https://doi.org/10.1109/TGRS.2017.2685945

Xing, C., Ma, L., Yang, X., 2016. Stacked Denoise Autoencoder Based Feature Extraction and Classification for Hyperspectral Images. J. Sens. 2016, 1–10. https://doi.org/10.1155/2016/3632943

Xu, X., Li, W., Ran, Q., Du, Q., Gao, L., Zhang, B., 2018. Multisource Remote Sensing Data Classification Based on Convolutional Neural Network. IEEE Trans. Geosci. Remote Sens. 56, 937–949. https://doi.org/10.1109/TGRS.2017.2756851

Yosinski, J., Clune, J., Nguyen, A., Fuchs, T., Lipson, H., 2015. Understanding Neural Networks Through Deep Visualization. ArXiv150606579 Cs.

Yu, Y., Gong, Z., Wang, C., Zhong, P., 2017. An Unsupervised Convolutional Feature Fusion Network for Deep Representation of Remote Sensing Images. IEEE Geosci. Remote Sens. Lett. 1–5. https://doi.org/10.1109/LGRS.2017.2767626

Yu, Y., Guan, H., Zai, D., Ji, Z., 2016. Rotation-and-scale-invariant airplane detection in high-resolution satellite images based on deep-Hough-forests. ISPRS J. Photogramm. Remote Sens. 112, 50–64. https://doi.org/10.1016/j.isprsjprs.2015.04.014

Yue, J., Zhao, W., Mao, S., Liu, H., 2015. Spectral–spatial classification of hyperspectral images using deep convolutional neural networks. Remote Sens. Lett. 6, 468–477. https://doi.org/10.1080/2150704X.2015.1047045

Zabalza, J., Ren, J., Zheng, J., Zhao, H., Qing, C., Yang, Z., Du, P., Marshall, S., 2016. Novel segmented stacked autoencoder for effective dimensionality reduction and feature extraction in hyperspectral imaging. Neurocomputing 185, 1–10. https://doi.org/10.1016/j.neucom.2015.11.044

Zeiler, M.D., Fergus, R., 2014. Visualizing and Understanding Convolutional Networks, in: Fleet, D., Pajdla, T., Schiele, B., Tuytelaars, T. (Eds.), Computer Vision – ECCV 2014: 13th European Conference, Zurich, Switzerland, September 6-12, 2014, Proceedings, Part I. Springer International Publishing, Cham, pp. 818–833. https://doi.org/10.1007/978-3-319-10590-1_53

Zeiler, M.D., Fergus, R., 2013. Visualizing and Understanding Convolutional Networks. ArXiv13112901 Cs.

Zhang, C., Pan, X., Li, H., Gardiner, A., Sargent, I., Hare, J., Atkinson, P.M., 2018a. A hybrid MLP-CNN classifier for very fine resolution remotely sensed image classification. ISPRS J. Photogramm. Remote Sens. 140, 133–144. https://doi.org/10.1016/j.isprsjprs.2017.07.014

Zhang, C., Sargent, I., Pan, X., Gardiner, A., Hare, J., Atkinson, P.M., 2018b. VPRS-Based Regional Decision Fusion of CNN and MRF Classifications for Very Fine Resolution Remotely Sensed Images. IEEE Trans. Geosci. Remote Sens. 56, 4507–4521. https://doi.org/10.1109/TGRS.2018.2822783

Zhang, C., Sargent, I., Pan, X., Li, H., Gardiner, A., Hare, J., Atkinson, P.M., 2018c. An object-based convolutional neural network (OCNN) for urban land use classification. Remote Sens. Environ. 216, 57–70. https://doi.org/10.1016/j.rse.2018.06.034

Zhang, F., Du, B., Zhang, L., 2017. A multi-task convolutional neural network for mega-city analysis using very high resolution satellite imagery and geospatial data. ArXiv170207985 Cs.

Zhang, Fan, Du, B., Zhang, L., 2016. Scene Classification via a Gradient Boosting Random Convolutional Network Framework. IEEE Trans. Geosci. Remote Sens. 54, 1793–1802. https://doi.org/10.1109/TGRS.2015.2488681

Zhang, F., Du, B., Zhang, L., 2015. Saliency-Guided Unsupervised Feature Learning for Scene Classification. IEEE Trans. Geosci. Remote Sens. 53, 2175–2184. https://doi.org/10.1109/TGRS.2014.2357078

Zhang, H., Li, Y., Zhang, Y., Shen, Q., 2017. Spectral-spatial classification of hyperspectral imagery using a dual-channel convolutional neural network. Remote Sens. Lett. 8, 438–447. https://doi.org/10.1080/2150704X.2017.1280200

Zhang, L., Shi, Z., Wu, J., 2015. A Hierarchical Oil Tank Detector With Deep Surrounding Features for High-Resolution Optical Satellite Imagery. IEEE J. Sel. Top. Appl. Earth Obs. Remote Sens. 8, 4895–4909. https://doi.org/10.1109/JSTARS.2015.2467377

Zhang, L., Zhang, L., Du, B., 2016. Deep Learning for Remote Sensing Data: A Technical Tutorial on the State of the Art. IEEE Geosci. Remote Sens. Mag. 4, 22–40. https://doi.org/10.1109/MGRS.2016.2540798

Zhang, Liangpei, Zhang, Lefei, Du, B., 2016. Deep Learning for Remote Sensing Data: A Technical Tutorial on the State of the Art. IEEE Geosci. Remote Sens. Mag. 4, 22–40. https://doi.org/10.1109/MGRS.2016.2540798

Zhao, C., Wan, X., Zhao, G., Cui, B., Liu, W., Qi, B., 2017. Spectral-Spatial Classification of Hyperspectral Imagery Based on Stacked Sparse Autoencoder and Random Forest. Eur. J. Remote Sens. 50, 47–63. https://doi.org/10.1080/22797254.2017.1274566

Zhao, W., Du, S., 2016. Learning multiscale and deep representations for classifying remotely sensed imagery. ISPRS J. Photogramm. Remote Sens. 113, 155–165. https://doi.org/10.1016/j.isprsjprs.2016.01.004

Zhao, W., Du, S., Emery, W.J., 2017. Object-Based Convolutional Neural Network for High-Resolution Imagery Classification. IEEE J. Sel. Top. Appl. Earth Obs. Remote Sens. 10, 3386–3396. https://doi.org/10.1109/JSTARS.2017.2680324

Zhao, W., Guo, Z., Yue, J., Zhang, X., Luo, L., 2015. On combining multiscale deep learning features for the classification of hyperspectral remote sensing imagery. Int. J. Remote Sens. 36, 3368–3379. https://doi.org/10.1080/2150704X.2015.1062157

Zhou, W., Newsam, S., Li, C., Shao, Z., 2017. Learning Low Dimensional Convolutional Neural Networks for High-Resolution Remote Sensing Image Retrieval. Remote Sens. 9, 489. https://doi.org/10.3390/rs9050489

Zhou, W., Shao, Z., Cheng, Q., 2016. Deep feature representations for high-resolution remote sensing scene classification, in: 2016 4th International Workshop on Earth Observation and Remote Sensing Applications (EORSA). Presented at the 2016 4th International Workshop on Earth Observation and Remote Sensing Applications (EORSA), pp. 338–342. https://doi.org/10.1109/EORSA.2016.7552825

Zhou, W., Shao, Z., Diao, C., Cheng, Q., 2015. High-resolution remote-sensing imagery retrieval using sparse features by auto-encoder. Remote Sens. Lett. 6, 775–783. https://doi.org/10.1080/2150704X.2015.1074756

Zhou, Y., Arpit, D., Nwogu, I., Govindaraju, V., 2014. Is Joint Training Better for Deep Auto-Encoders? ArXiv14051380 Cs Stat.

Zhu, X., Goldberg, A.B., 2009. Introduction to Semi-Supervised Learning. Synth. Lect. Artif. Intell. Mach. Learn. 3, 1–130. https://doi.org/10.2200/S00196ED1V01Y200906AIM006

Zhu, X.X., Tuia, D., Mou, L., Xia, G.-S., Zhang, L., Xu, F., Fraundorfer, F., 2017. Deep Learning in Remote Sensing: A Comprehensive Review and List of Resources. IEEE Geosci. Remote Sens. Mag. 5, 8–36. https://doi.org/10.1109/MGRS.2017.2762307

Zou, Q., Ni, L., Zhang, T., Wang, Q., 2015. Deep Learning Based Feature Selection for Remote Sensing Scene Classification. IEEE Geosci. Remote Sens. Lett. 12, 2321–2325. https://doi.org/10.1109/LGRS.2015.2475299

# *Appendix A*

Table A1: Database of collected deep network application in remote sensing

| | | *Other network parameters* | | *Dataset specification* | | | | *Best reported performances* | | |
|---|---|---|---|---|---|---|---|---|---|---|
| *Reference* | *Network Type* | *# of parameters* | *Learning type* | *Dataset* | *Spatial resolution* | *# of channels* | *Training proportion* | *Metric type* | *Deep network* | *SVM (Non deep)* |
| (Penatti et al., 2015) | CNN | 289M | Transfer learning | Brazilian coffee | | 3 | 0.8 | Average accuracy | 83 | 87 |
| (Yu et al., 2017) | CNN | 24.6M | Unsupervised | Brazilian coffee | | 3 | 0.8 | Overall accuracy | 87.8 | 87 |
| (Castellucci o et al., 2015) | CNN | 5M | Transfer learning | Brazilian coffee | | 3 | | Overall accuracy | 91.8 | |
| (Nogueira et al., 2017) | CNN | 60M | Transfer learning & fine-tuning | Brazilian coffee | | 3 | 0.6 | Overall accuracy | 94.5 | 87 |
| (Wu and Prasad, 2018) | CNN+RNN | | Semisupervised | Houston | 2.5 m | 144 | | Overall accuracy | 82.6 | 80.2 |
| (Xu et al., 2018) | CNN | | Supervised+ | Houston | 2.5 m | 144+1 | 0.19 | Overall accuracy | 88 | 80.5 |
| (Pan et al., 2018) | CNN | | | Houston | 2.5 m | 144 | | Overall accuracy | 90.8 | |
| (Li et al., 2014) | DBN | 14.7K | Unsupervised & fine-tuning | Houston | 2.5 m | 144 | | Overall accuracy | 97.7 | 97.5 |
| (Zabalza et al., 2016) | SAE | 4.2K | Unsupervised | Indian Pines | 20 m | 200 | 0.05 | Overall accuracy | 80.7 | 82.1 |
| (Ghamisi et al., 2016) | CNN | 188K | Supervised | Indian Pines | 20 m | 200 | 0.05 | Overall accuracy | 83.3 | 78.2 |
| (Shi and Pun, 2018) | CNN | 2.5M | Supervised | Indian Pines | 20 m | 200 | 0.01 | Overall accuracy | 85.2 | |
| (Mou et al., 2018b) | CNN | 1.44M | Unsupervised & fine-tuning | Indian Pines | 20 m | 200 | 0.05 | Overall accuracy | 85.8 | 72.8 |
| (C. Zhao et al., 2017) | SAE | 30.2K | Unsupervised & fine-tuning | Indian Pines | 20 m | 200 | 0.1 | Overall accuracy | 89.8 | 88.9 |
| (W. Hu et al., 2015) | CNN | 80.6K | Supervised | Indian Pines | 20 m | 220 | 0.2 | Overall accuracy | 90.2 | 87.6 |
| (Pan et al., 2018) | CNN | | | Indian Pines | 20 m | 200 | | Overall accuracy | 90.7 | |
| (Xing et al., 2016) | SAE | 241K | Unsupervised | Indian Pines | 20 m | 200 | 0.5 | Overall accuracy | 92.1 | 90.6 |
| (W. Li et al., 2017) | CNN | 57.9K | Supervised | Indian Pines | 20 m | 220 | 0.2 | Overall accuracy | 94.3 | 88.2 |
| (Chen et al., 2015) | DBN | | Unsupervised & fine-tuning | Indian Pines | 20 m | 200 | 0.5 | Overall accuracy | 96 | 95.5 |
| (Li et al., 2015) | SAE | 21.7M | Unsupervised & fine-tuning | Indian Pines | 20 m | 200 | 0.05 | Overall accuracy | 96.3 | 92.4 |
| (Sun et al., 2017) | SAE | 107K | Semisupervised | Indian Pines | 20 m | 200 | 0.1 | Overall accuracy | 96.4 | 80.6 |

| | | | | | | | | | | |
|---|---|---|---|---|---|---|---|---|---|---|
| (Ding et al., 2017) | CNN | 380K | Unsupervised | Indian Pines | 20 m | 200 | 0.5 | Overall accuracy | 97.8 | |
| (Ma et al., 2015) | SAE | 14.2K | Unsupervised & fine-tuning | Indian Pines | 20 m | 200 | 0.1 | Overall accuracy | 98.2 | |
| (Paoletti et al., 2018) | CNN | 96M | Supervised | Indian Pines | 20 m | 200 | 0.24 | Overall accuracy | 98.4 | |
| (Chen et al., 2016) | CNN | 44.9M | Supervised | Indian Pines | 20 m | 200 | 0.2 | Overall accuracy | 98.5 | 96.9 |
| (H. Zhang et al., 2017) | CNN | | Supervised | Indian Pines | 20 m | 200 | 0.1 | Overall accuracy | 98.8 | |
| (Makantasis et al., 2015) | CNN | 97.6K | Supervised | Indian Pines | 20 m | 224 | 0.8 | Overall accuracy | 98.9 | 82.7 |
| (Y. Li et al., 2017) | CNN | 197K | Supervised | Indian Pines | 20 m | 200 | 0.5 | Overall accuracy | 99.1 | |
| (Haut et al., 2018) | CNN | 8.9M | Supervised+ | Indian Pines | 20 m | 200 | 0.5 | Overall accuracy | 99.8 | 81.3 |
| (Sherrah, 2016) | CNN | 3.26M | Supervised | ISPRS Potsdam | 5 cm | 5 | 0.45 | Overall accuracy | 84.1 | |
| (Volpi and Tuia, 2017) | CNN | 6.38M | Supervised | ISPRS Potsdam | 5 cm | 5 | 0.45 | Overall accuracy | 85.8 | |
| (Maggiori et al., 2016) | CNN | 530K | Supervised | ISPRS Potsdam | 5 cm | 4 | 0.45 | Overall accuracy | 87 | |
| (Zhang et al., 2018a) | CNN | 17K | Supervised | ISPRS Potsdam | 5 cm | 4 | 0.75 | Overall accuracy | 89.4 | 82.4 |
| (Sherrah, 2016) | CNN | 22.7M | Transfer learning & fine-tuning | ISPRS Potsdam | 5 cm | 4 | 0.45 | Overall accuracy | 90.3 | |
| (Yongcheng Liu et al., 2018) | CNN | 481M | Transfer learning & fine-tuning | ISPRS Potsdam | 5 cm | 4 (DSMs not used) | 0.63 | Overall accuracy | 91.1 | |
| (Tschannen et al., 2016) | CNN | 30K | Supervised | ISPRS Vaihingen | 9 cm | 5 | 0.3 | Overall accuracy | 85.5 | |
| (Paisitkriangkrai et al., 2015) | CNN | | Supervised | ISPRS Vaihingen | 9 cm | 5 | 0.3 | Overall accuracy | 86.9 | |
| (W. Zhao et al., 2017) | CNN | | Supervised | ISPRS Vaihingen | 9 cm | 4 | 0.1 | Overall accuracy | 87.1 | 66.6 |
| (Volpi and Tuia, 2017) | CNN | 6.38M | Supervised | ISPRS Vaihingen | 9 cm | 4 | 0.3 | Overall accuracy | 87.3 | |
| (Marcos et al., 2018) | CNN | 100K | Supervised | ISPRS Vaihingen | 9 cm | 4 | 0.45 | Overall accuracy | 87.6 | |
| (Zhang et al., 2018b) | CNN | 17K | Supervised | ISPRS Vaihingen | 9 cm | 4 | 0.7 | Overall accuracy | 88.4 | 81.7 |
| (Maggiori et al., 2016) | CNN | 727K | Supervised | ISPRS Vaihingen | 9 cm | 4 | 0.3 | Overall accuracy | 88.9 | |
| (Sherrah, 2016) | CNN | 3.26M | Supervised | ISPRS Vaihingen | 9 cm | 4 | 0.3 | Overall accuracy | 89.1 | |
| (Audebert et al., 2016) | CNN | 32M | Transfer learning & fine-tuning | ISPRS Vaihingen | 9 cm | 4 | 0.3 | Overall accuracy | 89.8 | |
| (Marmanis et al., 2016b) | CNN | 806M | Transfer learning & fine-tuning | ISPRS Vaihingen | 9 cm | 4 | 0.3 | Overall accuracy | 90.3 | |

| | | | | | | | | | | |
|---|---|---|---|---|---|---|---|---|---|---|
| (Yongcheng Liu et al., 2018) | CNN | 481M | Transfer learning & fine-tuning | ISPRS Vaihingen | 9 cm | 3 (DSMs not used) | 0.47 | Overall accuracy | 91.1 | |
| (C. Zhao et al., 2017) | SAE | 20.8K | Unsupervised & fine-tuning | Kennedy Space Center | 18 m | 224 | 0.1 | Overall accuracy | 93.5 | 91.1 |
| (Chen et al., 2016) | CNN | 5.85M | Supervised | Kennedy Space Center | 18 m | 224 | 0.1 | Overall accuracy | 97.1 | 95.7 |
| (Y. Chen et al., 2014) | SAE | 8.72K | Unsupervised & fine-tuning | Kennedy Space Center | 18 m | 176 | 0.6 | Overall accuracy | 98.8 | 98.7 |
| (Haut et al., 2018) | CNN | 8.8M | Supervised+ | Kennedy Space Center | 18 m | 224 | 0.85 | Overall accuracy | 100 | 94.4 |
| (Ishii et al., 2015) | CNN | 60M | Supervised | Landsat 8 | 30m | 3 | 0.35 | F1 | 71 | 37.2 |
| (Mou et al., 2018a) | CNN+RNN | | Supervised | Landsat ETM | 30 m | 6 | | Overall accuracy | 98 | 95.7 |
| (Karalas et al., 2015) | SAE | 155K | Unsupervised & fine-tuning | MODIS | 500 sq.m | 7 | | Average precision | 62.8 | |
| (Zhou et al., 2017) | CNN | 126M | Transfer learning & fine-tuning | Other | 0.5m | 3 | | ANMRR | 0.04 | |
| (Kemker et al., 2018) | CNN | 11.9M | Supervised+ | Other | 4.7 cm | 6 | 0.25 | Average accuracy | 57.3 | 29.6 |
| (Kemker et al., 2018) | CNN | 69M | Supervised+ | Other | 4.7 cm | 6 | 0.25 | Average accuracy | 59.8 | 29.6 |
| (Bittner et al., 2017) | CNN | 134M | Transfer learning & fine-tuning | Other | 0.5m | 1 | | F1 | 70 | |
| (Lagrange et al., 2015) | CNN | 141M | Transfer learning | Other | 5 cm | 4 | 0.6 | Overall accuracy | 72.4 | 70.2 |
| (Cao et al., 2016) | CNN | 60M | Transfer learning & fine-tuning | Other | | 3 | | F1 | 72.4 | |
| (Ji et al., 2018) | CNN | 102K | Supervised+ | Other | 15 m | 4 | 0.85 | Overall accuracy | 79.4 | 78.5 |
| (Fu et al., 2017) | CNN | | Supervised | Other | 1m | 3 | 0.9 | F1 | 79.5 | 61.5 |
| (Tang et al., 2017) | CNN | | Transfer learning & fine-tuning | Other | | 3 | | Average precision | 79.5 | |
| (Huang et al., 2018) | CNN | 39M | Transfer learning & fine-tuning | Other | 0.5 m | 4 | 0.57 | Overall accuracy | 80 | 71.8 |
| (Chen et al., 2018) | CNN | | Transfer learning & fine-tuning | Other | 8 , 16 m | 3 | | Average precision | 80 | |
| (Chen et al., 2013) | DBN | 4.2M | Unsupervised & fine-tuning | Other | | 3 | 0.2 | F1 | 81.7 | 78.4 |
| (Marcos et al., 2018) | CNN | 430K | Supervised | Other | 5 cm | 4 | 0.7 | Overall accuracy | 82.6 | |
| (Cheng et al., 2017b) | CNN | 14.7M | Transfer learning | Other | 30m | | 0.2 | Overall accuracy | 84.3 | |
| (Yanfei Liu et al., 2018) | CNN | | Supervised | Other | 4 m (MSI), 1 m (Pan) | 3 | 0.8 | Overall accuracy | 85 | 84.7 |
| (Yongcheng Liu et al., 2018) | CNN | 481M | Transfer learning & fine-tuning | Other | 1 m | 3 | 0.93 | F1 | 85.6 | |
| (Geng et al., 2015) | SAE | 28.4K | Unsupervised & fine-tuning | Other | 0.38m | 1 | 0.5 | Overall accuracy | 88.1 | 76.9 |

| | | | | | | | | | | |
|---|---|---|---|---|---|---|---|---|---|---|
| (Lguensat et al., 2017) | CNN | 177K | Supervised | Other | | 1 | 0.18 | Overall accuracy | 88.6 | |
| (Han et al., 2018) | CNN | 286M | Semisupervised | Other | 30m | | | Overall accuracy | 88.6 | |
| (Zhao et al., 2015) | DBN | 379K | Unsupervised & fine-tuning | Other | 0.6m | 1 | 0.7 | Overall accuracy | 88.9 | 85.6 |
| (Zhang et al., 2018c) | CNN | 226K | Supervised | Other | 50 cm | 4 | 0.6 | Overall accuracy | 89.5 | 79.5 |
| (Zhang et al., 2018a) | CNN | 17K | Supervised | Other | 50 cm | 4 | 0.5 | Overall accuracy | 89.6 | |
| (Zhang et al., 2018b) | CNN | 17K | Supervised | Other | 50 cm | 4 | 0.7 | Overall accuracy | 89.8 | 81.2 |
| (Vakalopoulou et al., 2015) | CNN | 60M | Transfer learning | Other | 0.6m | 4 | 0.4 | Average precision | 90 | |
| (Qayyum et al., 2017) | CNN | 6.61M | Transfer learning | Other | 15cm | 3 | 0.8 | Overall accuracy | 90.3 | 83.1 |
| (Cheng et al., 2017a) | CNN | 134M | Transfer learning & fine-tuning | Other | 30m | | 0.8 | Overall accuracy | 90.3 | |
| (F. Zhang et al., 2015) | SAE | 90.3K | Unsupervised | Other | 1 m | 3 | 0.25 | Overall accuracy | 90.8 | 90 |
| (Zhang et al., 2018a) | CNN | 17K | Supervised | Other | 50 cm | 4 | 0.5 | Overall accuracy | 90.9 | |
| (Zhang et al., 2018c) | CNN | 226K | Supervised | Other | 50 cm | 4 | 0.6 | Overall accuracy | 90.9 | 80.4 |
| (Zhang et al., 2018b) | CNN | 17K | Supervised | Other | 50 cm | 4 | 0.7 | Overall accuracy | 91 | 81.7 |
| (Zhao and Du, 2016) | CNN | | Supervised | Other | 1.8m | 8 | 0.15 | Overall accuracy | 91.1 | |
| (Huang et al., 2018) | CNN | 39M | Transfer learning & fine-tuning | Other | 1.24 m | 8 | 0.62 | Overall accuracy | 91.3 | 80 |
| (Khan et al., 2017) | CNN | 151M | Transfer learning & fine-tuning | Other | 25m | 3 | 0.9 | Overall accuracy | 91.3 | 76.5 |
| (Han et al., 2018) | CNN | 286M | Semisupervised | Other | | | | Overall accuracy | 91.4 | |
| (X. Chen et al., 2014) | CNN | 395K | Supervised | Other | | 1 | | F1 | 91.6 | 79.3 |
| (L. Zhang et al., 2015) | CNN | 44M | Transfer learning | Other | | 3 | 0.75 | F1 | 91.8 | |
| (Khan et al., 2017) | CNN | 151M | Transfer learning & fine-tuning | Other | 25m | 3 | 0.9 | Overall accuracy | 92 | 74.1 |
| (F. Zhang et al., 2017) | CNN | 266K | Supervised | Other | 1.2 m | 3 | 0.8 | Overall accuracy | 92.4 | |
| (Pan et al., 2018) | CNN | | | Other | 1 m | 84 | | Overall accuracy | 93.2 | |
| (S. Liu et al., 2018) | CNN | 28.4M | Transfer learning & fine-tuning | Other | | 3 | 0.67 | Overall accuracy | 93.4 | 78 |
| (Basu et al., 2015) | DBN | 3.6K | Unsupervised & fine-tuning | Other | | 4 | 0.8 | Overall accuracy | 93.9 | |
| (Längkvist et al., 2016) | CNN | 1.91M | Unsupervised & fine-tuning | Other | 0.5 m | 6 | 0.7 | Overall accuracy | 94.5 | |
| (Ji et al., 2018) | CNN | 102K | Supervised+ | Other | 4 m | 4 | 0.17 | Overall accuracy | 94.7 | 93.5 |

| | | | | | | | | | | |
|---|---|---|---|---|---|---|---|---|---|---|
| (Rezaee et al., 2018) | CNN | 53.9M | Transfer learning & fine-tuning | Other | 5 m | 5 (3 used for CNN) | 0.46 | Overall accuracy | 94.8 | |
| (Cui et al., 2018) | CNN | 9.7K | Supervised | Other | 2m (MSI), 0.5m (Pan) | 8 (MSI) + Pan | 0.8 | Overall accuracy | 94.8 | |
| (Yanfei Liu et al., 2018) | CNN | | Supervised | Other | 2 m | 3 | 0.8 | Overall accuracy | 94.8 | 80.3 |
| (Xing et al., 2016) | SAE | 52.8K | Unsupervised | Other | 30 m | 224 | 0.5 | Overall accuracy | 95.5 | 96.9 |
| (Gong et al., 2017) | SAE | 81K | Unsupervised & fine-tuning | Other | 2m | 4 | 0.5 | Overall accuracy | 95.7 | 94.4 |
| (Ma et al., 2016) | CNN | | Supervised | Other | | 4 | 0.8 | Overall accuracy | 96 | |
| (W. Zhao et al., 2017) | CNN | | Supervised | Other | 0.5 m | 8 | 0.1 | Overall accuracy | 96.3 | 66.5 |
| (Han et al., 2018) | CNN | 286M | Semisupervised | Other | | 3 | | Overall accuracy | 96.8 | |
| (Hu et al., 2017) | CNN | | Supervised | Other | 1m | 161 | | Overall accuracy | 97 | 93.6 |
| (Yu et al., 2016) | DBN | 2.43M | Unsupervised & fine-tuning | Other | 0.27m | 3 | | F1 | 97 | |
| (Wu and Prasad, 2018) | CNN+RNN | | Semisupervised | Other | 1 m | 360 | | Overall accuracy | 97.3 | 95.2 |
| (Wang et al., 2018) | CNN | 252K | Supervised | Other | | 3 | 0.74 | Overall accuracy | 97.3 | 93.7 |
| (Basu et al., 2015) | DBN | 3.6K | Unsupervised & fine-tuning | Other | | 4 | 0.8 | Overall accuracy | 97.9 | |
| (Xu et al., 2018) | CNN | | Supervised+ | Other | 1 m | 63+1 | 0.03 | Overall accuracy | 97.9 | 92.7 |
| (Nogueira et al., 2017) | CNN | 5M | Transfer learning & fine-tuning | Other | 0.5 m | 3 | 0.6 | Overall accuracy | 98 | 90 |
| (Tao et al., 2018) | CNN | | Supervised | Other | 0.5 ~ 4 m | 4 | 0.008 | Overall accuracy | 98.4 | 89.2 |
| (Ma et al., 2016) | CNN | | Supervised | Other | | 4 | 0.8 | Overall accuracy | 98.4 | |
| (Gong et al., 2018) | CNN | 139M | Transfer learning & fine-tuning | Other | 2 m | 3 | 0.8 | Overall accuracy | 98.5 | 77.7 |
| (Wang et al., 2015) | CNN | 438K | Supervised | Other | | 3 | 0.6 | Overall accuracy | 98.7 | |
| (Fan Zhang et al., 2016) | CNN | | Supervised | Other | 1 m | 3 | 0.2 | Overall accuracy | 98.8 | |
| (Weng et al., 2018) | CNN | 3.4M | Transfer learning | Other | | | 0.25 | Overall accuracy | 98.8 | 91.3 |
| (Gong et al., 2018) | CNN | 139M | Transfer learning & fine-tuning | Other | | 3 | 0.8 | Overall accuracy | 98.8 | |
| (Ji et al., 2018) | CNN | 107K | Supervised+ | Other | 4 m | 4 | 0.03 | Overall accuracy | 98.9 | 96.5 |
| (Maggiori et al., 2017) | CNN | 459K | Supervised | Other | 1 m | 3 | 0.9 | Overall accuracy | 99.5 | 94.9 |
| (Y. Li et al., 2017) | CNN | 128K | Supervised | Other | 30 m | 242 | 0.5 | Overall accuracy | 99.6 | |
| (Basaeed et al., 2016) | CNN | 56.4K | Supervised | Other | 30m | 10 | 0.75 | Overall accuracy | 99.7 | |

| | | | | | | | | | | |
|---|---|---|---|---|---|---|---|---|---|---|
| (Weng et al., 2018) | CNN | 3.4M | Transfer learning | Other | | | 0.5 | Overall accuracy | 99.7 | |
| (W. Zhao et al., 2017) | CNN | | Supervised | Pavia Center | 1.3 m | 103 | 0.1 | Overall accuracy | 96.3 | 92.98 |
| (Shi and Pun, 2018) | CNN | 673K | Supervised | Pavia Center | 1.3 m | 103 | 0.001 | Overall accuracy | 97 | |
| (Aptoula et al., 2016) | CNN | 1.31M | Supervised | Pavia Center | 1.3 m | 103 | 0.05 | Kappa | 97.4 | |
| (Zabalza et al., 2016) | SAE | 2.4K | Unsupervised | Pavia Center | 1.3 m | 103 | 0.05 | Overall accuracy | 97.4 | 97.4 |
| (Ben Hamida et al., 2018) | CNN | 3681 | Supervised | Pavia Center | 1.3 m | 103 | 0.05 | Overall accuracy | 98.9 | |
| (Tao et al., 2015) | SAE | | Unsupervised | Pavia Center | 1.3 m | 103 | 0.05 | Overall accuracy | 99.6 | |
| (Zhao and Du, 2016) | CNN | | Supervised | Pavia Center | 1.3 m | 103 | 0.05 | Overall accuracy | 99.7 | 97.7 |
| (Makantasis et al., 2015) | CNN | 10.9K | Supervised | Pavia Center | 1.3 m | 103 | 0.8 | Overall accuracy | 99.9 | 99 |
| (Ghamisi et al., 2016) | CNN | 188K | Supervised | Pavia University | 1.3 m | 103 | 0.1 | Overall accuracy | 83.4 | 78.2 |
| (Mou et al., 2018b) | CNN | 1.39M | Unsupervised & fine-tuning | Pavia University | 1.3 m | 103 | 0.1 | Overall accuracy | 87.4 | 79.9 |
| (Wu and Prasad, 2018) | CNN+RNN | | Semisupervised | Pavia University | 1.3 m | 103 | | Overall accuracy | 88.4 | 81.2 |
| (Ding et al., 2017) | CNN | 226K | Unsupervised | Pavia University | 1.3 m | 100 | 0.5 | Overall accuracy | 90.6 | |
| (W. Hu et al., 2015) | CNN | 80.6K | Supervised | Pavia University | 1.3 m | 103 | 0.05 | Overall accuracy | 92.6 | 90.5 |
| (Yue et al., 2015) | CNN | 182K | Supervised | Pavia University | 1.3 m | 103 | | Overall accuracy | 95.2 | 85.2 |
| (Xing et al., 2016) | SAE | 212K | Unsupervised | Pavia University | 1.3 m | 103 | 0.5 | Overall accuracy | 96 | 93.6 |
| (Zhao et al., 2015) | CNN | 239K | Unsupervised | Pavia University | 1.3 m | 103 | 0.1 | Overall accuracy | 96.4 | 85.2 |
| (W. Li et al., 2017) | CNN | 57.9K | Supervised | Pavia University | 1.3 m | 103 | 0.05 | Overall accuracy | 96.5 | 90.6 |
| (Zhao and Du, 2016) | CNN | | Supervised | Pavia University | 1.3 m | 103 | 0.1 | Overall accuracy | 96.8 | 80.1 |
| (Ben Hamida et al., 2018) | CNN | 6862 | Supervised | Pavia University | 1.3 m | 103 | 0.05 | Overall accuracy | 97.2 | |
| (Paoletti et al., 2018) | CNN | 173M | Supervised | Pavia University | 1.3 m | 103 | 0.04 | Overall accuracy | 97.8 | |
| (Aptoula et al., 2016) | CNN | 1.31M | Supervised | Pavia University | 1.3 m | 103 | 0.1 | Kappa | 97.9 | |
| (Shi and Pun, 2018) | CNN | 673K | Supervised | Pavia University | 1.3 m | 103 | 0.01 | Overall accuracy | 98.5 | |
| (Y. Chen et al., 2014) | SAE | 29K | Unsupervised & fine-tuning | Pavia University | 1.3 m | 103 | 0.6 | Overall accuracy | 98.5 | 97.4 |

| | | | | | | | | | | |
|---|---|---|---|---|---|---|---|---|---|---|
| (Tao et al., 2015) | SAE | | Unsupervised | Pavia University | 1.3 m | 103 | 0.1 | Overall accuracy | 98.6 | |
| (Ma et al., 2015) | SAE | 10K | Unsupervised & fine-tuning | Pavia University | 1.3 m | 103 | 0.1 | Overall accuracy | 98.7 | |
| (Sun et al., 2017) | SAE | 30.2K | Semisupervised | Pavia University | 1.3 m | 103 | 0.1 | Overall accuracy | 98.7 | 91.1 |
| (Xu et al., 2018) | CNN | | Supervised+ | Pavia University | 1.3 m | 103 | 0.04 | Overall accuracy | 99.1 | 89.9 |
| (Chen et al., 2015) | DBN | | Unsupervised & fine-tuning | Pavia University | 1.3 m | 103 | 0.5 | Overall accuracy | 99.1 | 98.4 |
| (Y. Li et al., 2017) | CNN | 110K | Supervised | Pavia University | 1.3 m | 103 | 0.5 | Overall accuracy | 99.4 | |
| (Makantasis et al., 2015) | CNN | 10.9K | Supervised | Pavia University | 1.3 m | 103 | 0.8 | Overall accuracy | 99.6 | 93.9 |
| (H. Zhang et al., 2017) | CNN | | Supervised | Pavia University | 1.3 m | 103 | 0.05 | Overall accuracy | 99.7 | |
| (Chen et al., 2016) | CNN | 5.85M | Supervised | Pavia University | 1.3 m | 103 | 0.1 | Overall accuracy | 99.7 | 97.7 |
| (Zhou et al., 2017) | CNN | 126M | Transfer learning & fine-tuning | RSSCN7 | | 3 | | ANMRR | 0.3 | |
| (Zou et al., 2015) | DBN | 3.1M | Unsupervised & fine-tuning | RSSCN7 | | 3 | 0.5 | Average accuracy | 77 | |
| (Wu et al., 2016) | SAE | 2.53M | Unsupervised | RSSCN7 | | 3 | 0.5 | Overall accuracy | 90.4 | |
| (W. Hu et al., 2015) | CNN | 80.6K | Supervised | Salinas | 3.7 m | 220 | 0.05 | Overall accuracy | 92.6 | 91.7 |
| (W. Li et al., 2017) | CNN | 57.9K | Supervised | Salinas | 3.7 m | 204 | 0.05 | Overall accuracy | 94.8 | 92.9 |
| (Xu et al., 2018) | CNN | | Supervised+ | Salinas | 3.7 m | 204 | 0.06 | Overall accuracy | 97.7 | 92.2 |
| (Ma et al., 2015) | SAE | 37.7K | Unsupervised & fine-tuning | Salinas | 3.7 m | 204 | 0.01 | Overall accuracy | 98.3 | |
| (Makantasis et al., 2015) | CNN | 10.9K | Supervised | Salinas | 3.7 m | 224 | 0.8 | Overall accuracy | 99.5 | 94 |
| (Haut et al., 2018) | CNN | 8.9M | Supervised+ | Salinas | 3.7 m | 204 | 0.5 | Overall accuracy | 99.9 | 91.1 |
| (Zhou et al., 2017) | CNN | 126M | Transfer learning & fine-tuning | UC Merced | 1 ft | 3 | | ANMRR | 0.33 | |
| (Zhou et al., 2015) | SAE | 51.6K | Unsupervised | UC Merced | 1 ft | 3 | | Average precision | 64.5 | |
| (F. Zhang et al., 2015) | SAE | 301K | Unsupervised | UC Merced | 1 ft | 3 | 0.8 | Overall accuracy | 82.7 | 81.7 |
| (Romero et al., 2016) | CNN | 49.1M | Unsupervised | UC Merced | 1 ft | 3 | 0.8 | Overall accuracy | 84.5 | |
| (Yu et al., 2017) | CNN | 24.6M | Unsupervised | UC Merced | 1 ft | 3 | 0.8 | Overall accuracy | 88.57 | 81.7 |
| (Marmanis et al., 2016a) | CNN | 155M | Transfer learning & fine-tuning | UC Merced | 1 ft | 3 | 0.7 | Overall accuracy | 92.4 | |
| (Wu et al., 2016) | SAE | 2.53M | Unsupervised | UC Merced | 1 ft | 3 | 0.5 | Overall accuracy | 92.7 | |

| | | | | | | | | | | |
|---|---|---|---|---|---|---|---|---|---|---|
| (Weng et al., 2017) | CNN | 60M | Transfer learning | UC Merced | 1 ft | 3 | 0.7 | Overall accuracy | 93.4 | |
| (Luus et al., 2015) | CNN | 920K | Supervised | UC Merced | 1 ft | 3 | 0.8 | Overall accuracy | 93.5 | |
| (Fan Zhang et al., 2016) | CNN | | Supervised | UC Merced | 1 ft | 3 | 0.8 | Overall accuracy | 94.5 | |
| (Han et al., 2018) | CNN | 286M | Semisupervised | UC Merced | 1 ft | 3 | | Overall accuracy | 94.5 | |
| (Yanfei Liu et al., 2018) | CNN | | Supervised | UC Merced | 1 ft | 3 | 0.8 | Overall accuracy | 95.6 | 92.9 |
| (Zhou et al., 2016) | CNN | 126M | Transfer learning & fine-tuning | UC Merced | 1 ft | 3 | 0.8 | Overall accuracy | 96.48 | 92.3 |
| (F. Hu et al., 2015) | CNN | 19.6M | Transfer learning | UC Merced | 1 ft | 3 | 0.8 | Overall accuracy | 96.9 | |
| (Castellucci o et al., 2015) | CNN | 5M | Transfer learning | UC Merced | 1 ft | 3 | | Overall accuracy | 97.1 | |
| (Gu et al., 2018) | CNN | 117M | Transfer learning | UC Merced | 1 ft | 3 | 0.8 | Overall accuracy | 97.1 | 81.7 |
| (Gong et al., 2018) | CNN | 139M | Transfer learning & fine-tuning | UC Merced | 1 ft | 3 | 0.8 | Overall accuracy | 98.3 | 77.4 |
| (Penatti et al., 2015) | CNN | 204M | Transfer learning | UC Merced | 1 ft | 3 | 0.8 | Average accuracy | 99.4 | 81 |
| (Nogueira et al., 2017) | CNN | 5M | Transfer learning & fine-tuning | UC Merced | 1 ft | 3 | 0.6 | Overall accuracy | 99.5 | 90 |
| (F. Hu et al., 2015) | CNN | 44.1M | Transfer learning | WHU-RS19 | | 3 | 0.6 | Overall accuracy | 98.6 | |